LONGITUDINAL VEHICLE SPEED CONTROLLER FOR AUTONOMOUS DRIVING IN URBAN STOP-AND-GO TRAFFIC SITUATIONS

A Thesis

Presented in Partial Fulfillment of the Requirements for

the Degree Master of Science in the

Graduate School of The Ohio State University

By

Neil R. Sawant, B. E.

Graduate Program in Electrical and Computer Engineering

* * * * *

The Ohio State University

2010

Master's Examination Committee

Prof. Umit A. Ozguner, Advisor

Prof. Kevin M. Passino

ABSTRACT

In this thesis, we have addressed the issue of road congestion due to increased traffic in urban and metropolitan areas and have designed an autonomous longitudinal speed controller as a solution to this problem. One of the best ways to increase efficiency of the available road infrastructure is to enable vehicles to move in a platoon with very small distance headway from the preceding vehicle. We have developed a Longitudinal Finite State Machine which acts as a supervisory control to help the following vehicle to merge behind and follow the preceding vehicle. We have studied the performance of two vehicle following controllers, i.e. LQR based full-state feedback controller and LQR based sequential-state feedback controller, which are enabled and take the control of the vehicle velocity during the "follow" state of the vehicle's Longitudinal FSM. A comparison analysis has been presented between the two controllers which help in reducing the distance headway from the preceding vehicle as well as maintaining string stability within the platoon.

This is dedicated to my parents, Ravi and Kamal Sawant, the best parents anyone can have in this world, my lovely and amazing sisters, Renu and Priya Tai and to all my friends who have stood by me and encouraged me throughout my life.

ACKNOWLEDGEMENTS

I am extremely grateful to God for giving me such a kind, encouraging, intellectual and supportive family. My parents have always been the ones showing me the right way and guiding me through the most important part of my childhood. It's only because of them that I have been able to reach this stage of my life and I believe that it could not have been better than this. My sister, Renu tai, has been such a powerful source of inspiration for me and I have not seen a women as strong, intelligent and accomplished as her at her age. I have grown older through my childhood with a hope of being as meticulous, thorough and hardworking as my oldest sister Priya tai.

This thesis would be incomplete without mentioning the selfless support I have received from my best friend, my brother Saahil. He has been with me through thick and thin and has always helped me stand taller and stronger. I want to thank Nimish, JD and Siddharth who are my closest friends for being a part of my life and I live each day with a hope of being around them in future without which life would be black and white. If there was anyone who helped me remain sane and supported me through the first one year after coming to US, it was Satty and I cannot thank him more. I am sure he will remember in what 'good' shape I was and how he 'rescued' my life! I am thankful to my roommates and friends Swanand 'Swanan' Phadke, Harshad 'Harry' Paranjape, Nisheet 'Betha'

Singh, Vivek ‘Mohammed’ Venkatachallam, Manjunath ‘Boobanath’ Reddy and all the people who ‘came’ and ‘went’ in my life after coming to US and have been a part of this amazing journey.

I am highly thankful to my advisor, Professor Umit A. Ozguner for accepting me in his research group and letting me do my thesis under his supervision. I feel highly obliged and grateful to him for giving me time and attention throughout the time I was at OSU. He has always made me think about a topic in depth and has encouraged me to work hard. After working hard through the first year he was kind and fair to me by offering me Research Assistantship and relieving the financial burden off my parents. Without his guidance, motivation and support this work would not have been possible.

Professor Vadim Utkin introduced me to modern controls and I feel extremely lucky to have been his student. But it was Professor Kevin M. Passino who made learning Control Systems so interesting and fun. He is one of the very few professors who makes a student to think on his own and develops an interest for the topic. He was the most approachable professor in OSU and I am extremely grateful to be associated with him.

I would also like to thank the Visiting Scholar, Dr. Naohisa Hashimoto, for his insights and elaborate discussions on various aspects of my thesis. His suggestions and encouragements have helped me a lot for writing my thesis.

This thesis was funded under the NSF Project, 0931669, on “CPS: Autonomous Driving in Mixed Traffic Urban Environments.” It was a very exciting topic to work on and I feel highly privileged to have been a part of it.

Finally, I thank God for his continued presence and blessing in my life and for giving me my inner strength.

VITA

January 4th 1986 ……... Born - Mumbai, Maharashtra,India

June 2007 ……..…… B.E Electronics

Sept 2009- Present …….. Graduate Research Associate,
Electrical and Computer Engineering Department,
The Ohio State University

June 2007 – Aug 2008 …….. Embedded Systems Engineer,
Lele Group of Companies, Mumbai, India

June 2007 – May 2008 …….. Visiting Faculty and Lab Instructor,
PVPP College of Engineering, Mumbai, India.

FIELDS OF STUDY

Major Field: Electrical & Computer Engineering

TABLE OF CONTENTS

LIST OF FIGURES

LIST OF TABLES

CHAPTER 1 INTRODUCTION

Many research groups are trying to solve the cooperative driving challenge. With increasing urban traffic and inadequacy in the infrastructure to support such large amount of traffic, a need arises for a change in paradigm to solve this problem. Safety, increased throughput, higher efficiency and decreased emissions are the main goals to be achieved and steps are being taken to solve these problems. The only solution to this problem seems to be the introduction of semi-automated vehicles to which are able to perform cooperate driving. Cooperative driving can be achieved by means of Vehicle-to-Vehicle (V2V) communication as shown in Figure 1. Existing infrastructure can be used in a more efficient way to facilitate improved behavior of individual vehicles.

Of course, automated vehicles cannot be commercialized at once and this has to be done in stages. Initially there will be a mixture of automated and semi-automated or fully manual operated vehicles. With public acceptance and further research, the goal of complete automated highway system may be achieved in near future.

The past efforts from the government include the Demo'97 conducted by the National Automated Highway System Consortium (NAHSC) which saw the use of Adaptive Cruise Control (ACC), Lane keeping and Obstacle/Collision Avoidance.

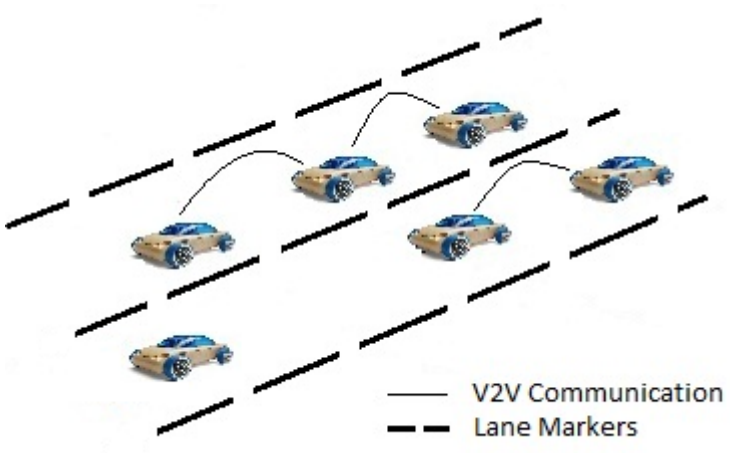

Figure 1: Driving in Urban Environment using V2V Communication

DARPA Grand Challenge was held in 2004 and 2005 and the DARPA Urban Challenge in 2007 in which the vehicles had to perform complex maneuvers like lane changing, passing and negotiating intersections.

1.1. Literature Overview and Car-Following Problem

For a completely automated highway and urban system, vehicles need to have extremely robust longitudinal and lateral controllers. The vehicles need to have robust sensing system which will be able to take high level control decisions for safe autonomous driving.

Car-following can be explained by the help of a simple scenario. Whenever we drive on a highway or a freeway, there is always a vehicle preceding our vehicle. It is more likely that the speed of the preceding vehicle is different than our speed. If we decide to follow the preceding vehicle we first try and reduce the headway distance to the desired time headway of 3 seconds. Then we try and match the speed of our vehicle to the speed of the preceding vehicle and once it is matched we continue to follow the

preceding vehicle with constant time headway. But as a human driver, we have a finite reaction time to sudden changes in the speed of the preceding vehicle in case it decides to suddenly accelerate or suddenly decelerate. This finite reaction time limits the following time headway to as large as 3 seconds. Decreasing it below 3 seconds would prove to be dangerous and may result in a collision. A controller can be developed which can allow smaller following time headways and which avoids collisions.

Also a phenomenon called stop waves or traffic shocks is prevalent in urban as well as highway traffic. A stop wave travels downstream the traffic and produces sustained oscillations which may result in collisions in a convoy of vehicles. So driver reaction time plays an important role in car-following. The car-following controller should also dampen the velocity oscillations produced by any car in the convoy maintaining string-stability. To handle this problem, a lot of research has been going on for developing robust car-following controllers.

The platooning or convoying problem has been one of the main research topics of many research groups. One of the earlier efforts by Bender-Fenton-Olson [1] produced results of longitudinal control of vehicles through road–side as well as vehicle-borne computers. Velocity control of the follower vehicle was done based on decreasing the velocity difference between the leader and follower vehicles using proportional type control law. The work by [2], [3] have made use of both lateral and longitudinal controllers to study lane changing and car-following problems. Longitudinal control of platoon was also studied by (Desoer, 1991) [4]. The control law used is a linear combination of velocity and acceleration perturbations over the

lead vehicle. Vehicle modeling and control as well as studies about platoon dynamics were seen in [5] and [6]. Hedrick *et. al.* [6] made use of Sliding mode control for controlling the follower vehicles in a platoon so as to achieve string stability. Simplified and computationally less expensive longitudinal vehicle model was developed my Martin Sommerville [7] as his master's thesis.

A number of developments were made using quadratic cost regulators. Levine *et. al.* [9] introduced an optimal linear state feedback controller to regulate the position and velocity of vehicles in a densely packed string of high-speed vehicles. Ozguner *et. al.* [10] modified the above theory to include sequential optimal linear state feedback from all the preceding vehicles to each vehicle in the sting to achieve asymptotic string stability.

1.2. Autonomous Vehicle and GCDC

In this thesis, an automated vehicle model is being investigated. This model has been in part taken from Martin Sommerville's master's thesis [7] in which he has modeled a 1992 Honda Accord, where the model was originally developed by Hatipoglu and Sommerville [18]. A few changes have been made to the controllers for better actuator response. Finite State Machine has been added to control the vehicle speed in different urban and highway scenarios. Also, longitudinal control has been implemented using two control techniques given in [9] and [10] in which LQR-based complete state-feedback and Ozguner's LQR-based sequential optimal state feedback control has been implemented to ensure asymptotic string stability in close car following.

GCDC stands for Grand Cooperative Driving Challenge and its aim is to facilitate the development and deployment of cooperative driving in urban as well as highway scenarios. It is a competition to be held in March 2011 which includes an urban task and a highway task to be completed by all participants.

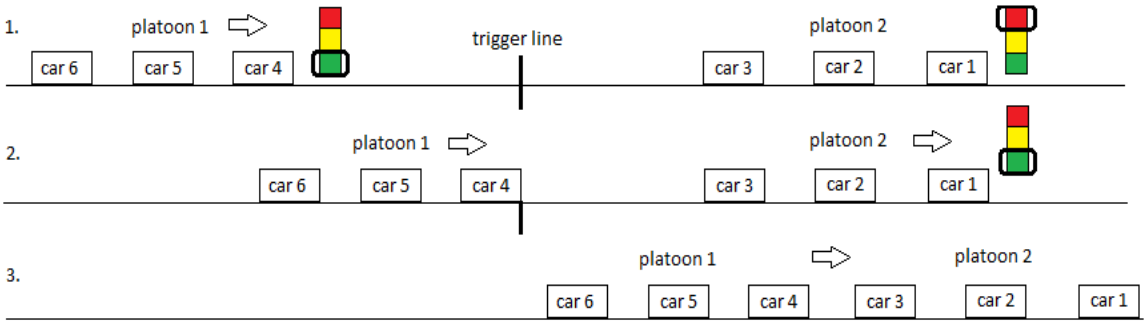

Figure 2 GCDC Urban Scenario

As shown in Figure 2, case 1, the urban task includes the convoy of vehicles (platoon 1) accelerating from rest as soon as a traffic signal goes green and smoothly reach and merge behind another convoy of vehicles (platoon 2) which has started from another traffic light preceding the first traffic light. The arrow shows the direction of motion. A team is formed by a set of two platoons starting one behind the other but each behind a traffic light. Two such teams of these platoons run side-by-side on parallel lanes. As shown in case 2, the green signal for platoon 2 of each team is triggered as soon as the first car of either of platoon 1 of the two teams passes a trigger line. As shown in case 3, the task for both the teams is to merge platoon 1 behind platoon 2 as smoothly as possible, while maintaining platoon stability. The last vehicle of any

team which crosses a check-point first gets a point for completing this task faster. Also teams which demonstrated dangerous driving may be penalized or disqualified.

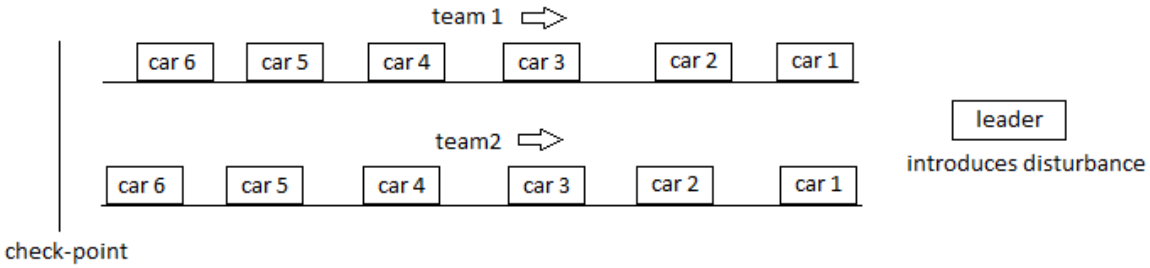

Figure 3 GCDC Highway Scenario

The highway task starts from where the urban task ends. A lead vehicle runs ahead of both the teams, as shown in Figure 3. A disturbance is introduced by a lead vehicle into both the convoys. The two teams/convoys should demonstrate string stability against external disturbance. Again the convoy which crosses the finish line first gets a point.

1.3.An Organizational Overview

The objective of this thesis is to present a control system which can optimally control a platoon of closely following vehicles for a stop-and-go type of traffic as illustrated in the GCDC scenarios. The platoon needs to demonstrate string stability and should be able to dampen any disturbance caused in any part of the platoon. A following distance of 4 meters or headway time of less than 1sec should be maintained between each vehicle in the platoon for stop-and-go situation.

In Chapter 2, three types of car models have been explained i.e. a simple drivetrain dynamics model also known as a point mass model, a non-linear vehicle dynamics

model from the work of Takasaki and Fenton [12] and the complex vehicle model from Martin Sommerville's thesis, which includes Engine Dynamics, Torque Convertor Dynamics, Transmission Dynamics as well as Drivetrain Dynamics. Simulation results for a step rise in reference velocity have also been provided.

In chapter 3, development of the FSM to control the vehicle in different states of approaching and following a vehicle has been explained.

In chapter 4, two types of car-following controllers i.e. LQR-based Complete State-feedback Controller and LQR-based Sequential State-feedback Controller have been explained. These controllers have been used on 6 vehicles and the simulation results for the two GCDC scenarios explained in section 1.2. have been provided.

CHAPTER 2 LONGITUDINAL VEHICLE MODELS

The longitudinal control problem has been divided into two aspects by D. F. Wilke [13] i.e. logical and control aspect. The logical aspect deals with deciding where the vehicle should be in future time step, given the current conditions, for best performance of the system. The control aspect deals with how the vehicles can be controlled to attain and maintain the desired position, while giving a comfortable and a safe ride as well as not exceeding the vehicle capabilities.

In order to be able to address the logical and control aspects of the longitudinal control problem, we need to have vehicle models which represent closely an actual vehicle behavior. In this chapter we are going to talk in brief about three types of longitudinal car models. A comparison study in form of simulations results for a step rise in reference velocity is provided in the end. The logical and the control aspects of the longitudinal control problem will be addressed in chapter 4. The three longitudinal car models are as mentioned below:

- Point-mass Model
- Non – linear Fenton – Takasaki Model
- Complete Vehicle Dynamics Sommerville – Hatipoglu Model[1]

[1] In each case the authors have integrated sub-models and concepts already known. Thus originality is not challenged.

2.1.Linear Longitudinal Vehicle Point-mass Model

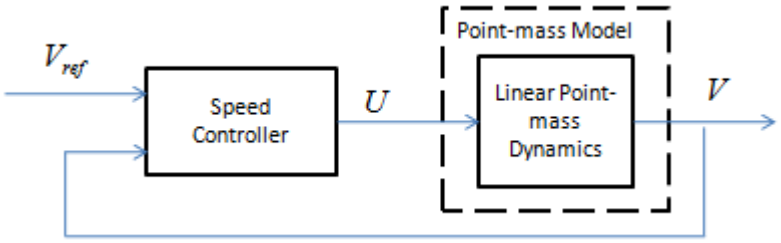

Figure 4 Point-mass Model

The point-mass longitudinal model of the vehicle is derived using Newton's 2nd law of motion. The net force acting on a vehicle is the algebraic sum of the drive force acting on the vehicle due to its propulsion system and the aerodynamic and frictional drag force which is a non-linear function the vehicle velocity. The model is as given below:

$$\dot{V} = \frac{1}{m}[-\alpha V + u]$$

where m = mass of the vehicle

V = longitudinal speed of the vehicle

α = linearized drag co-efficient acting upon the vehicle assuming small deviations from the desired speed.

u = drive force acting upon the vehicle through the control system.

Thus the transfer function for the above model would be as shown in Figure 5.

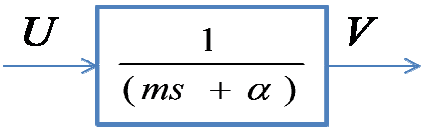

Figure 5 Point-mass Model Transfer Function

Where $V(s) = s\,X(s)$, the Laplace transforms of vehicle velocity and the distance traveled by it.

2.2.Non-Linear Longitudinal Vehicle Fenton-Takasaki Model

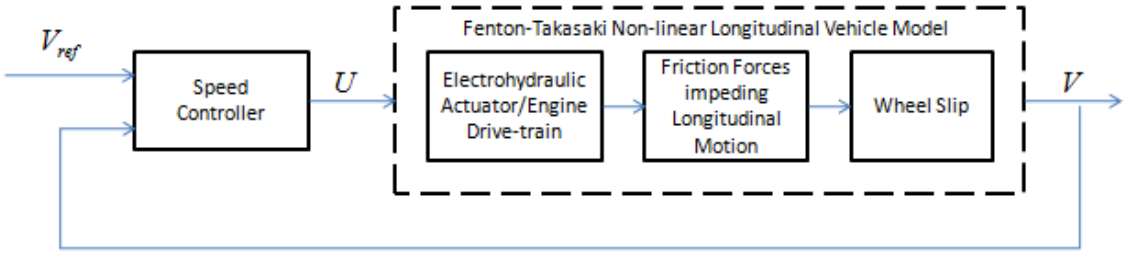

Figure 6 Fenton-Takasaki Model [14]

The point-mass model is inadequate to represent the true behavior of the car as it is valid for small-signal conditions around a certain operating point. Also, such models neglect the non-linearities as well as the complexities of the propulsion/combustion systems and of torque convertor dynamics if present. In practice, one would want to use a model which responds correctly to large-signal inputs which would make a stationary vehicle to accelerate to highways speeds as well as to decelerate from highway speeds to a complete halt, as required during urban driving.

Takasaki and Fenton [14] used a 1969 Plymouth sedan for the full-scale testing and estimation of a non-linear model of the vehicle which can be used to develop an

automatic longitudinal control under non-braking conditions. The model developed from field test data is valid for higher accelerations and is given as

$$V = \left[\frac{k_p(V)}{t_p(V)s+1}\right]\left[\frac{1}{s+0.05}\right]\left[\frac{\xi(V)}{s+\xi(V)}\right]U$$

where U = voltage applied to an electrohydraulic actuator, which controls the position of throttle valve

V = speed of the vehicle with respect to fixed reference frame

$k_p(V)$ = velocity dependent model parameter associated with throttle actuator and the propulsion systems

$t_p(V)$ = velocity dependent model parameter associated with this system as well as its interaction with the roadway interface

$\xi(V)$ = velocity dependent model parameter associated with the interaction of the system with the roadway interface.

$s = d/dt$

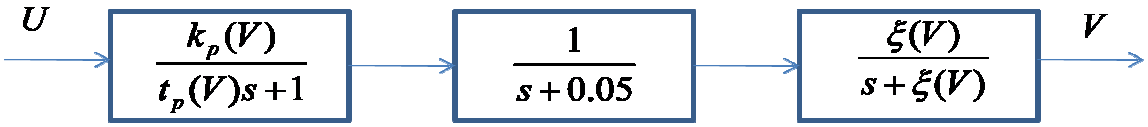

Figure 7 Empirically validated model of vehicle longitudinal dynamics

The model shown above has three blocks. The left-most block corresponds to the dynamics of electrohydraulic actuator/engine-drivetrain combustion. The middle block which contains a very slow pole corresponds to the friction forces which impede the longitudinal motion of the vehicle. The right-most block accounts for the effects of wheel slip. The terms $k_p(V), t_p(V)$ and $\xi(V)$ are non-linear functions of velocity and are shown in Figure 8 (a) and (b).

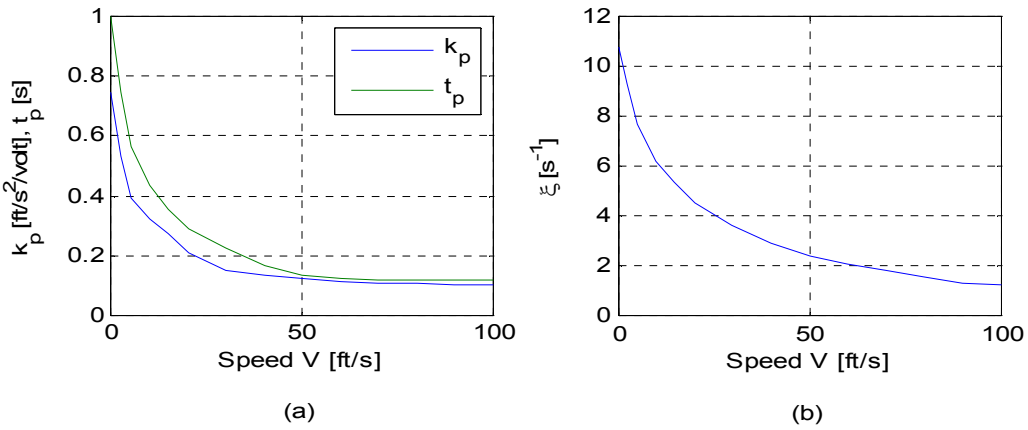

Figure 8 (a) k_p (V) and t_p (V), (b) ξ(V), empirically developed functions associated with derived dynamics

2.3.Complete Vehicle Dynamics Sommerville-Hatipoglu Model

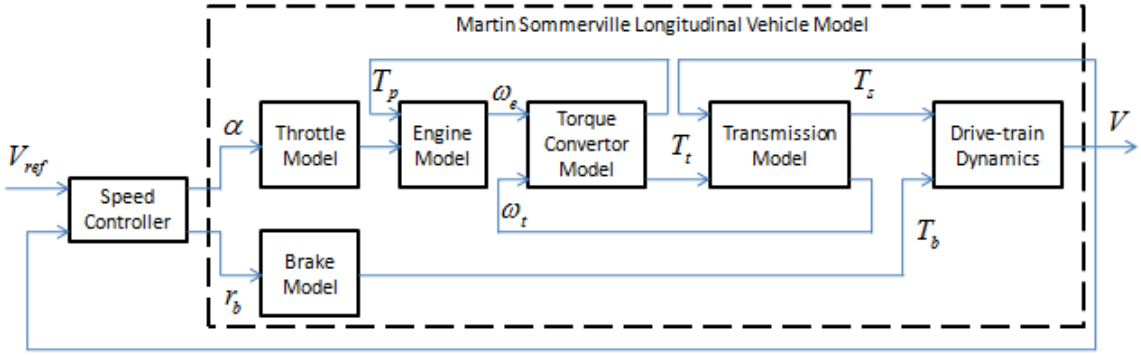

Figure 9 Sommerville-Hatipoglu's Longitudinal Vehicle Model

The vehicle model developed by Martin Sommerville and C. Hatipoglu [7], [18] has been explained in brief in Appendix A. The vehicle drive-train dynamics model is as given below.

$$\dot{V} = \frac{r}{M_v}(G_T T_t(\omega_e, \omega_t) - \gamma V^2 - T_{rr} - T_b)$$

Please refer to Appendix A for explanation of the variables used. Here, Newton's 2nd law of motion is applied to derive the above equation. The first term in the right hand side of the equation is the driving torque produced by the engine as well as the torque convertor, after the appropriate gear reduction, which drives the vehicle, the second term is the torque due to the aerodynamic drag acting on the vehicle due to its motion, the thirds term is the torque due to the rolling resistance produced by the road-tire interface and the fourth term is the breaking torque acting on the vehicle in case of deceleration.

The Fenton-Takasaki model did take care of the non-linear vehicle dynamics arising due to the propulsion/combustion system, torque convertor as well as the wheel slip. Also, the model is valid only in non-braking conditions. Sommerville-Hatipoglu developed a model of a 1992 Honda Accord which accounted for the engine dynamics, torque convertor dynamics, transmission and the drive-train dynamics. He also created the throttle and brake actuator models. This makes it possible for us to use this model for a thorough study of logical as well as control aspect of longitudinal vehicle following and control problem.

2.4. Simulation of the Three Longitudinal Models

The simulation results of the three models explained above, against a step rise in reference velocity, have been provided in Figure 10. The initial velocity for the vehicle simulated for all the models is zero. From Figure 10, we can see that point-mass model as well as the Takasaki-Fenton model does not show any gear change and torque convertor dynamics. The Sommerville-Hatipoglu model goes through 4 gear changes before it reaches 45mph. The steady state error of all three models is approximately

zero, same as the overshoot. From Figure 11, we can see that there are spikes in acceleration of the Sommerville-Hatipoglu model due to gear changes which is as expected. These spikes are produced due to the torque convertor at each gear change as there is a difference in the turbine as well as the pump speed when the gear changes. The spikes may be higher than that seen in the actual vehicle due to the modeling error of torque convertor.

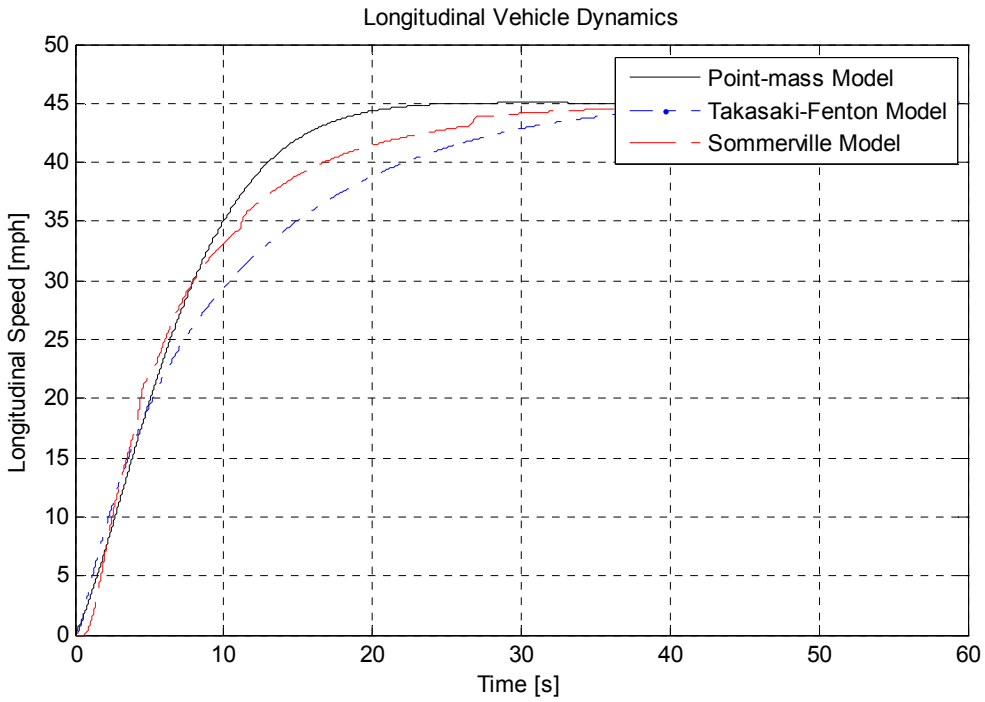

Figure 10 Simulation results of the three models explained above for a step rise of 45mph

The acceleration profiles for the above simulations are as shown in Figure 11.

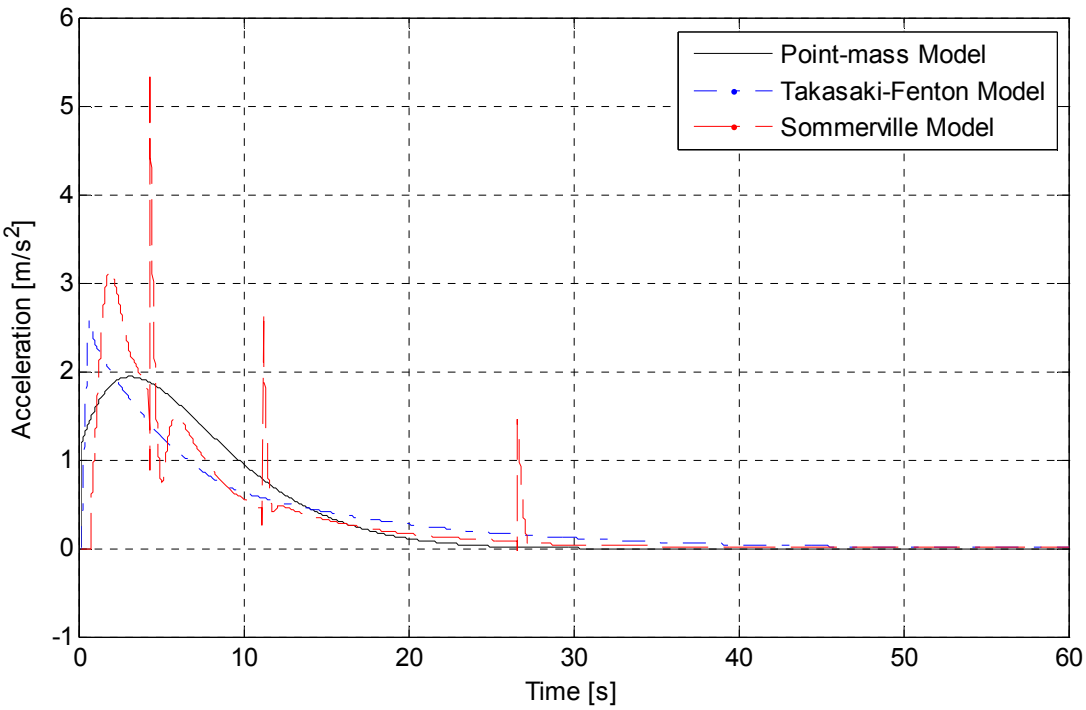

Figure 11 Acceleration of the vehicle models

As the Sommerville-Hatipoglu car model is the best and the most accurate representation of an actual Honda Accord vehicle, we will be using his model for our further simulation studies.

CHAPTER 3 LONGITUDINAL SPEED CONTROL USING A FINITE STATE MACHINE

The capacity of an Automated Highway System is calculated by the following formula:

$$C = \frac{V}{X_r + L}$$

where $C =$ is the capacity measured in number of vehicles crossing a fixed point/unit time

$V =$ vehicle speed of flow

$X_r =$ inter-vehicular spacing

$L =$ vehicle length.

The aim of a longitudinal vehicle speed controller is to maximize the capacity by efficiently utilizing the available infrastructure [15]. Capacity is the maximum possible flow-rate for a given speed V, inter-vehicular spacing X_r and vehicle length L. Due to the unpredictable urban traffic conditions, the flow-rate may exceed maximum allowable capacity C at certain instants of time by either exceeding maximum allowable vehicle speed V or minimum allowable inter-vehicular spacing X_r. The job of the speed controller is to limit the number of these excursions of the flow rate to a minimum with highest priority given to passenger safety. Also, the speed controller should be robust enough so that the flow-rate should converge to the maximum capacity C at steady-state.

In doing so, a supervisory speed controller needs to work over the vehicle following longitudinal speed controller to ensure that the above constraints are satisfied. Also, before the actual platooning stage, there are other stages where the following vehicle spots the leader and when it is within the sensing range it decides to merge behind it and follow it. These stages need to be handled by the supervisory control. This controller should also handle the emergency braking situation where the inter-vehicular distance is dangerously less than a threshold value.

The speed controller developed in [7] was not equipped to handle stop-and-go type urban traffic conditions. We want to develop a robust longitudinal controller which can limit the acceleration and deceleration of the vehicles within the desired limit of the competition. The desired limits of the competition are mentioned in table1.

Characteristic	**Specification**
Velocity	[0 to 80] km/h
Maximum Acceleration (a_{max})	2.0 m/s^2
Maximum Acceleration at least	1.5 m/s^2
Maximum Deceleration (a_{min})	-4.5 m/s^2
Maximum Deceleration at least	-4.0 m/s^2

Table 1. Maximum and Minimum Allowable Accelerations for the GCDC Competition.

Two approaches were used to develop controllers for close car following or for the distance headway following:

a. LQR-based Full State-feedback Longitudinal Control

b. LQR-based Sequential State-feedback Longitudinal Control

The complete longitudinal speed controller is as shown in fig. 12. The vehicle speed, inter-vehicular distance and inter-vehicular speed difference are the inputs to this supervisory controller. The platoon reference speed is received from the platoon leader. The on-board sensors provide the relative distance and relative speed of the preceding vehicle when it is in the sensing range and the V2V communication is used to receive the speeds as well as the positions of the other vehicles in the platoon. The on-board sensors can be used in combination with the V2V communication for sensor fusion for better accuracy as well as in case of communication failure as an emergency back-up.

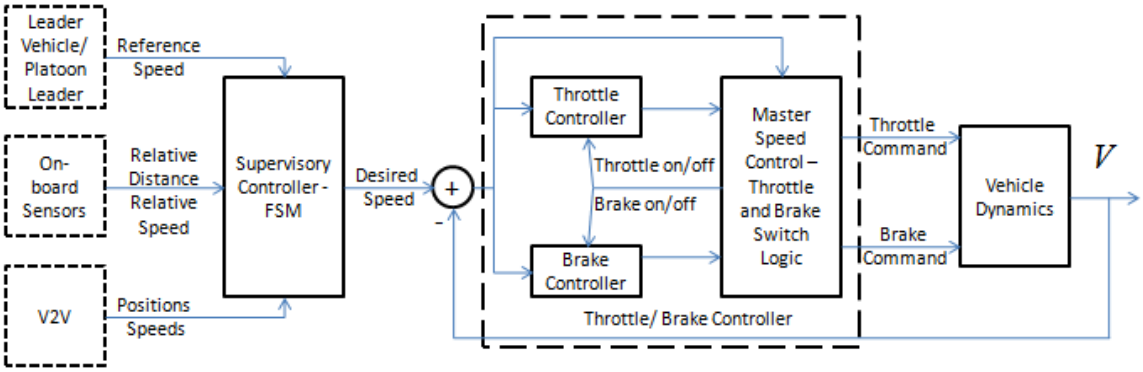

Figure 12 Block Diagram of Longitudinal Speed Controller

For the implementation of the supervisory control, we have developed a longitudinal FSM which controls the desired speed of the vehicle in different states of a merging as well as a platooning maneuver. An FSM is the best way to deal with the above maneuvers as a follower vehicle goes through different distinct states before it gets locked into following the leader vehicle. Each of these states requires a different control

to be implemented on the follower vehicle for smoothly merging and following the leader vehicle. The FSM is as explained below.

Longitudinal FSM:

A longitudinal FSM is used to control the desired speed of vehicles in a convoy in different stages of a vehicle following maneuver. The FSM switches from one state to the other using a rule base which is pre-defined. The supervisory controller has a "state select logic" block which decides which state to enter depending upon the inputs to it. The block diagram of the supervisory controller is as shown in fig. 12.

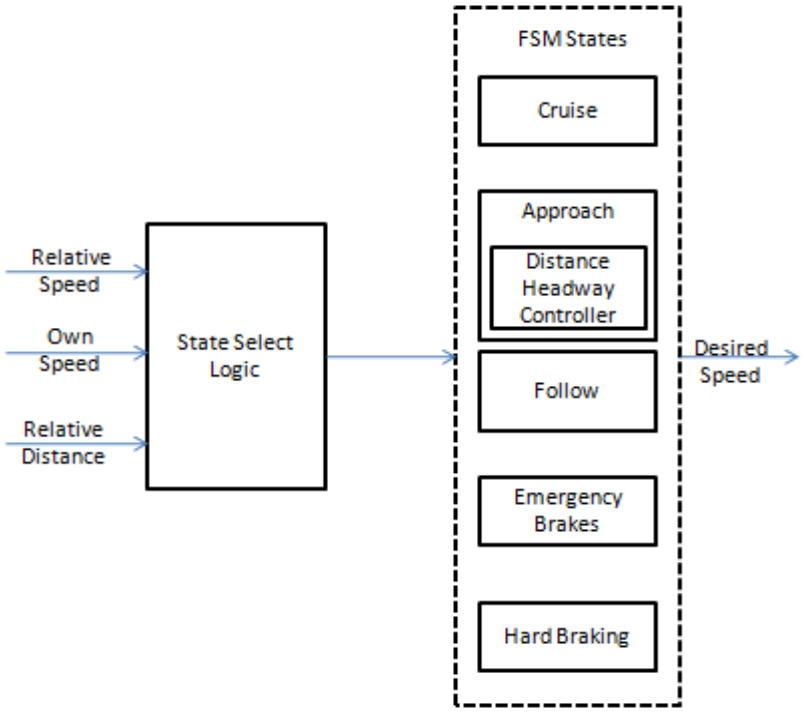

Figure 13 Block Diagram for Supervisory Controller

The states used in the FSM developed are mentioned in fig. 13. Also, the list of symbols used in the rest of chapter is mentioned below:

V = speed of the subject vehicle also referred to as the follower vehicle

V_{des}= desired velocity of the subject vehicle

V_{urban} = speed limit within the urban limits

$V_{highway}$ = speed limit on the highway

V_{leader} = speed of the preceding vehicle also referred to as the leader

val_1 = reduction of speed in Emergency Brakes State

val_2 = reduction of speed in Hard Braking State

$Leader$ = distance between the subject vehicle and its preceding vehicle

d_{sensor} = the sensing range of the subject vehicle beyond which the preceding vehicle cannot be sensed

d_{follow} = the minimum distance required for the subject vehicle to start following the preceding vehicle

d_{des} = desired following distance between the subject vehicle and its preceding vehicle

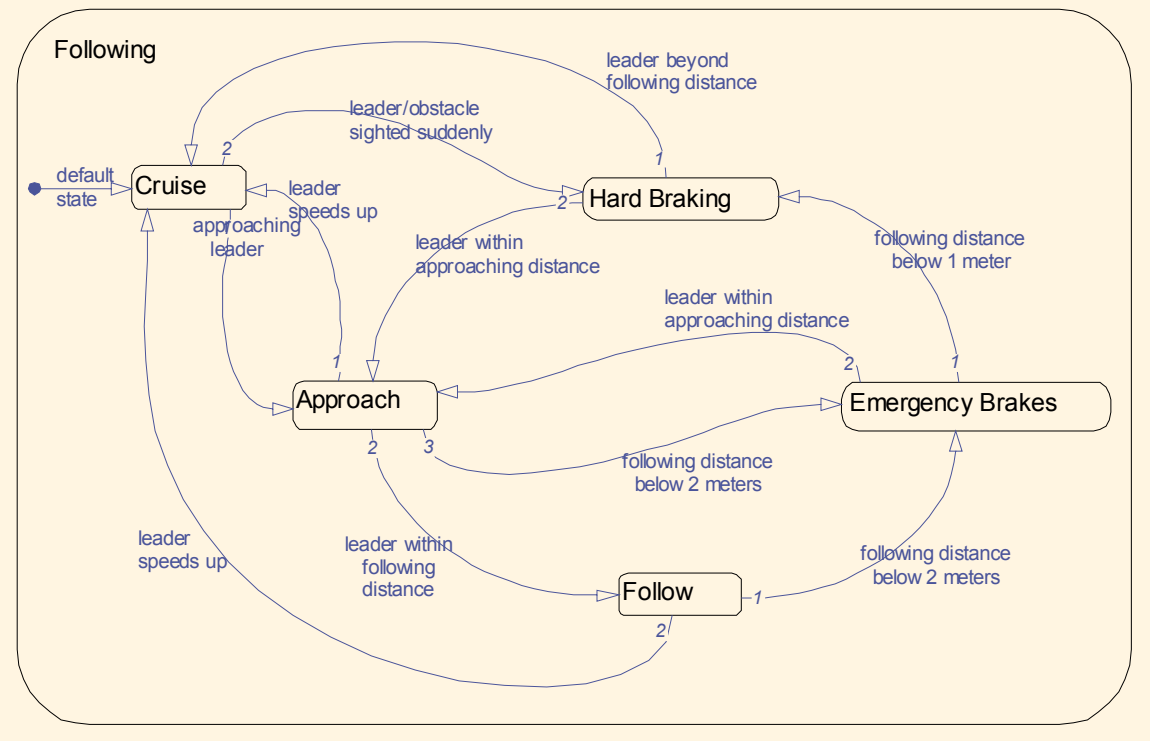

Figure 14 Finite State Machine

Each state is explained below

3.1.Cruise State

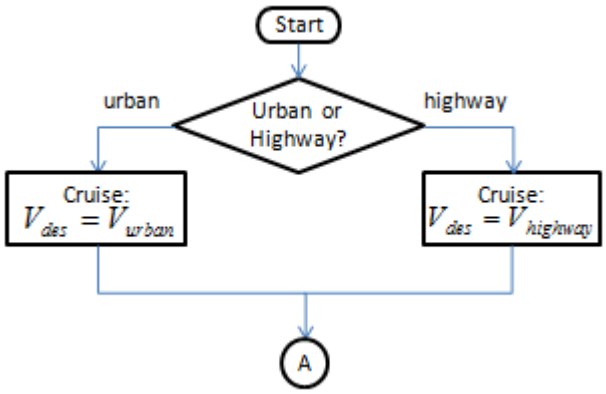

Figure 15 Cruise State

This is the default state from which any vehicle starts it motion. The flow chart representation for this state is shown in fig.14. The reference speed in this state is decided by the location of the vehicle, i.e. urban or highway. The cruise speed used is 25 mph if the vehicle is within the urban limits. The cruise speed is 45 mph if the vehicle is beyond the urban limits and on a highway. Only two situations have been considered here as is the requirement of the GCDC competition. One important task of the supervisory controller is to find out whether the vehicle is following another vehicle or whether the vehicle is a leader itself and an appropriate reference velocity should be assigned to it. This task is taken care by the cruise state.

3.2.Approach State

A vehicle enters this state only if it cites a leader within the approaching limits. The approaching limit is set to $d_{sensor} = 90\,m$ as the maximum sensing distance of a RADAR sensor is 106 m whereas of a LIDAR is 80 m.

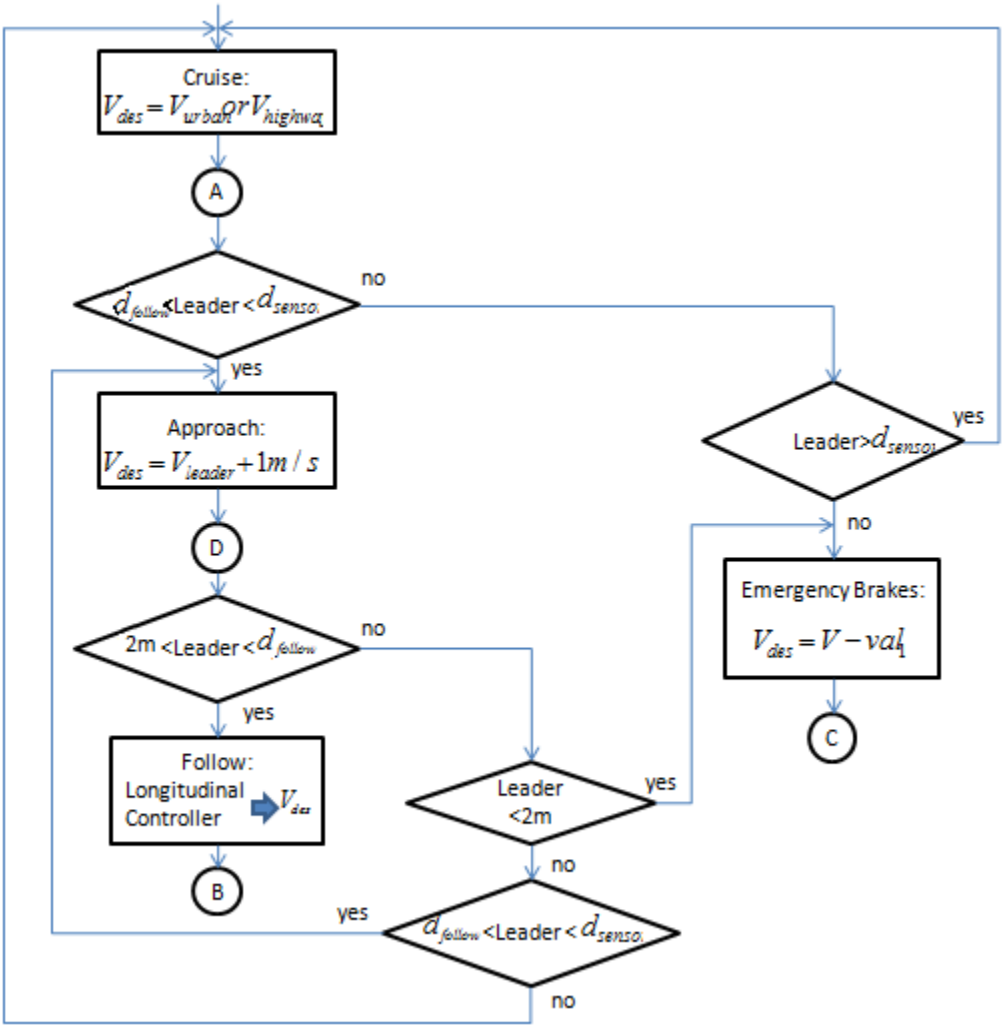

Figure 16 Approach State

In this state, the follower keeps its velocity slightly higher than the leader so that it can approach it smoothly. We have used the increment of 1 m/s for our simulations. In this case a velocity following maneuver is performed by Approach state keeping the velocity of the vehicle slightly higher than its leader velocity so that their relative distance decreases with every time step. If the distance of the leader becomes less than 1.5m, we enter the Emergency Brake state which is explained in section 3.4. If

the preceding vehicle accelerates at a rate higher than the allowable limit of $2m/s^2$ and goes beyond the sensing range of the subject vehicle, the Cruise state is entered.

3.3.Follow State

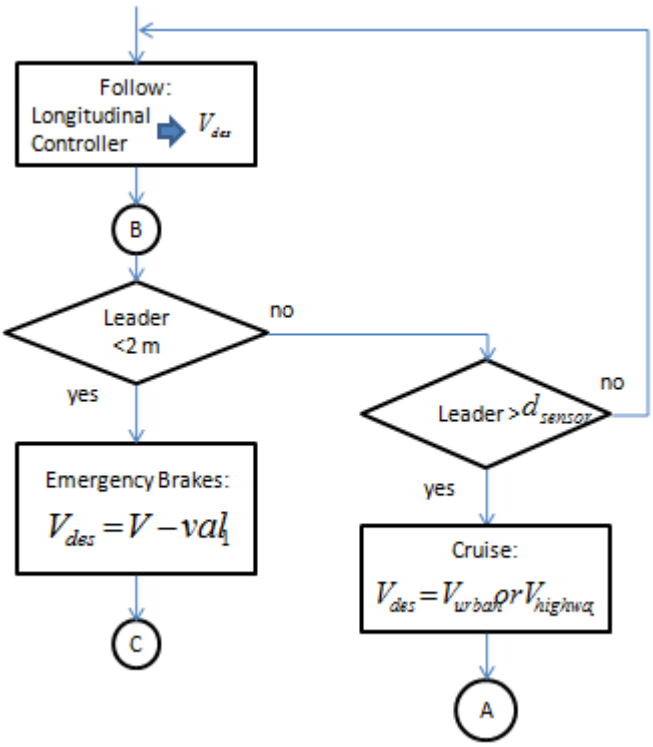

Figure 17 Follow State

The follower vehicle enters this state when it is within the following distance d_{follow} of the preceding vehicle. This distance is chosen to be 8.5 m for our simulations. The follower will try and further reduce the gap between the leader and itself till it reduces to a threshold value d_{des}. This value is chosen to be 4 m for our simulations. In this state one of the two controllers, explained in chapter 4 will be used. This state executes the distance headway following maneuver. If the distance from the leader reduces below 1.5m then Emergency Brake State is entered. In case

the leader accelerates and its distance increases beyond d_{sensor}, then the cruise state is entered.

3.4.Emergency Brake State

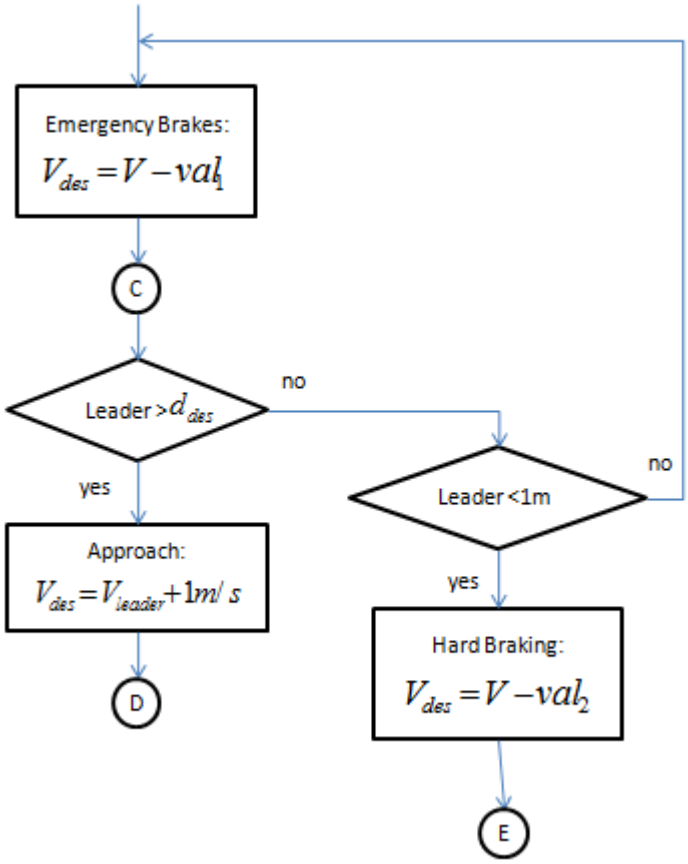

Figure 18 Emergency Brakes State

The follower vehicle enters this state if the following distance becomes too low. The threshold used in the simulations is 1.5 m. In this state, the desired velocity of the follower vehicle is set val_1 m/s less than that of its leader and is set to reduce by val_2 m/s at with every simulation time step. We have taken $val_1 = 1$ m/s for our simulations. This decelerates the follower and thus increases the following distance to

a safe value. If the following distance decreases below 0.5m, then the Hard Braking State is entered which is explained in the next section.

3.5.Hard Braking State

In this state, the follower vehicle comes dangerously close to the leader vehicle. In this case a hard deceleration is used to increase the following distance to a safe value.

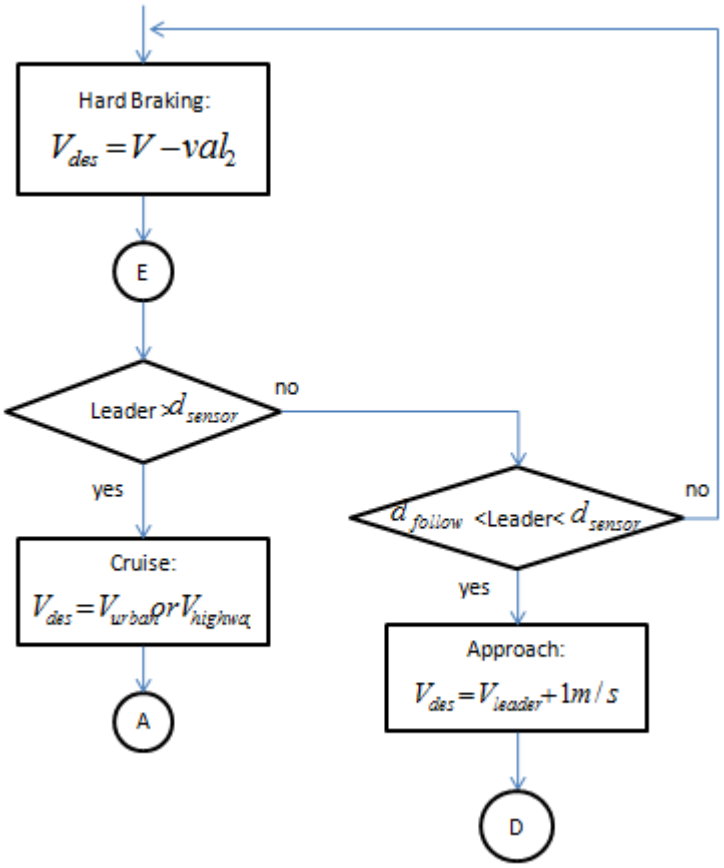

Figure 19 Hard Braking State

The threshold used for the simulations is 0.5 m. The desired velocity of the follower is set val_2 m/s less than that of its leader and is set to reduce by val_2 m/s at with every simulation time step. We have taken $val_2 = 2$ m/s for our simulations. During

deceleration of the vehicle, if the leader goes through higher accelerations and goes beyond the sensing distance d_{sensor}, the vehicle enters the Cruise State. If the distance of the leader goes beyond the following distance d_{follow} but is within the sensing distance d_{sense}, the vehicle enters the Approach State.

Now, let us see a 2-car "Approach and Match Speed – Fixed Headway" scenario and track the change of states on the FSM as shown in Figure 20**.** Here a follower vehicle starts 465 m from behind leader vehicle, which is at rest, and triggers the leader vehicle once it crosses a trigger line which is 85 m behind the leader.

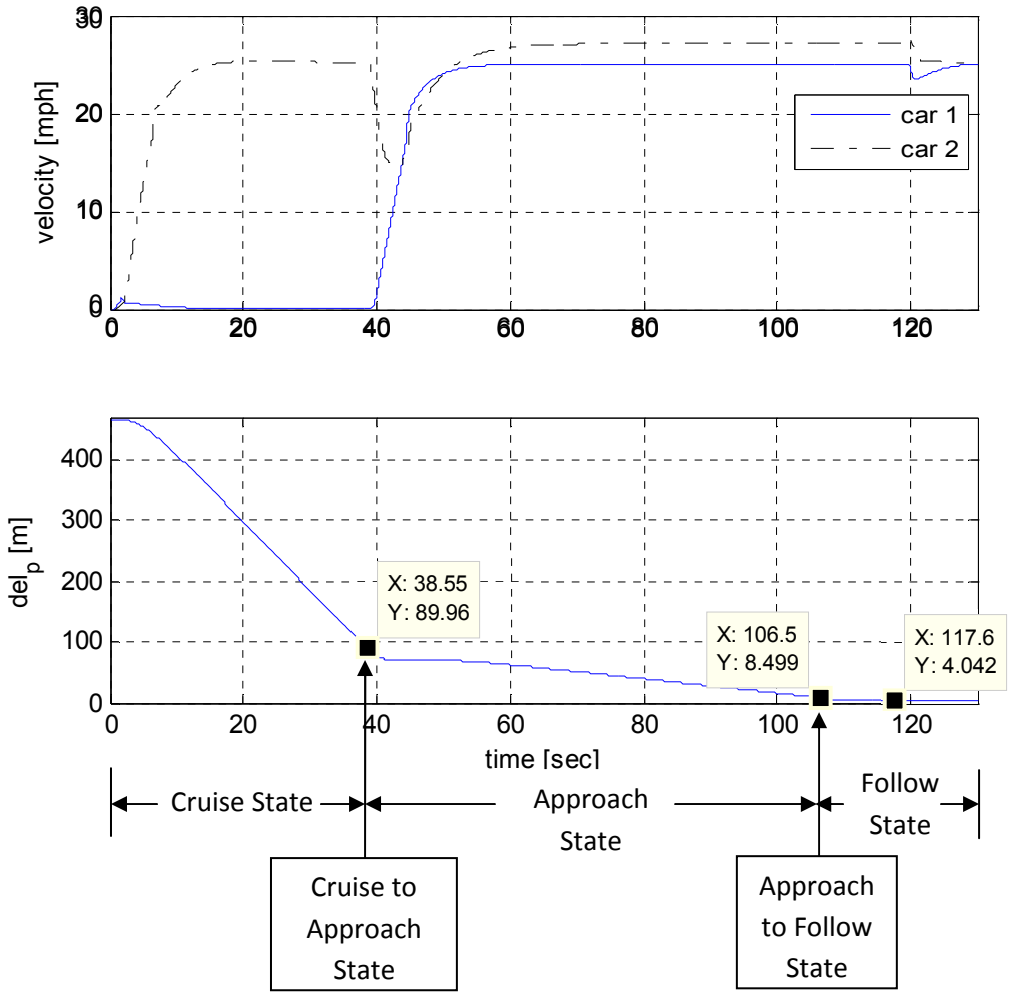

Figure 20 FSM State Transition in a Approach and Follow Maneuver

From

Figure **20**, we can see that the follower vehicle transitions from the Cruise state into the Approach state after the following distance is reduces below 90 m. Another State Transition occurs when the following distance reduces below 8.5 m from Approach state to Follow State. In the Follow state the following distance keeps reducing till it reaches the desired following distance of 4 m.

With the understanding of the vehicle model and the supervisory control, we can now move to the development of the close-following or distance-headway following controller used in the Follow State in the next chapter.

CHAPTER 4 GCDC SIMULATIONS

In 1962, major initiative was taken to improve the existing ground transportation system and an interest was generated for the introduction of high-speed ground transportation system (HSGT) for the Northeast Corridor (i.e. the region between Boston, MA. and Washinton, D.C.) [16]. These efforts were taken by the U.S. Department of Commerce after a proposal from a inter-disciplinary group from Massachusetts Institute of Technology. During this research program, the research teams from M.I.T. started developing research plans to take care of the basic research problems of scheduling, control, propulsion, vehicle and tube aerodynamics, and guideway problems. As a result of this research program, initial study on control of velocity and spacing of vehicles both on a single line and in merging situations was undertaken by Levine and Athans [9]. A few years later, more mature and practically feasible approach to the same problem was introduced by Ozguner and Perkins [10]. In this chapter, we are going to use the controllers developed in [9] and [10] on the complex car model of a 1992 Honda Accord developed in [7] which are going to work with the supervisory controller which we have developed in Chapter 3. The purpose of this thesis is to be able to study and compare the

results of the implementation of the above controllers on the complex vehicle model and to come up with an optimal control system that can be used in the GCDC competition.

Before we provide the simulation results for the two GCDC cases explained in Chapter 1, let us one by one talk about the two control strategies to be used for the close following maneuver.

4.1.LQR-based Full-state Feedback Controller

Consider a set of N linear, time-invariant systems represented by the following set of equations:

$$s_i : \dot{x}_i = A_i x_i + B_i u_i + B_{i+1} y_{i+1}$$

$$y_i = C_i x_i$$

where $i = 1, 2, \dots, N-1$ and $x_i \in R^n$, $u_i \in R^m$,$A_i \epsilon R^{n \times n}$ and $B_i \epsilon R^{n \times m}$.

$$s_N : \dot{x}_N = A_N x_N + B_N u_N$$

$$y_N = C_N x_N$$

where $x_N \in R^{n1}$, $u_N \in R^{m1}$,$A_N \epsilon R^{n1 \times n1}$ and $B_N \epsilon R^{n1 \times m1}$. Here $n \neq n1$.

To formulate the optimization problem, the system equations written above are written in such a way as to interlace the states of the systems as shown below:

$$\underbrace{\begin{bmatrix} \dot{x}_1 \\ \dot{x}_2 \\ \vdots \\ \dot{x}_N \end{bmatrix}}_{\dot{X}} = \underbrace{\begin{bmatrix} A_1 & B_2C_2 & 0 & 0 \\ 0 & A_2 & B_3C_3 & 0 \\ \vdots & \vdots & \ddots & \vdots \\ 0 & 0 & 0 & A_N \end{bmatrix}}_{A} \underbrace{\begin{bmatrix} x_1 \\ x_2 \\ \vdots \\ x_N \end{bmatrix}}_{X} + \underbrace{\begin{bmatrix} B_1 & 0 & 0 & 0 \\ 0 & B_2 & 0 & 0 \\ \vdots & \vdots & \ddots & \vdots \\ 0 & 0 & 0 & B_N \end{bmatrix}}_{B} \underbrace{\begin{bmatrix} u_1 \\ u_2 \\ \vdots \\ u_N \end{bmatrix}}_{U}$$

The above differential equation is of the form

$$\dot{X} = AX + BU$$

where components of vector $X = col[x_1\ x_2 \dots x_N]$

and that of vector $U = col[u_1\ u_2\ \ldots u_N]$.

For the solution of the above system to be optimal, the cost function to be minimized is defined as given below:

$$J = \frac{1}{2}\int_0^\infty \{X'QX + U'RU\}dt$$

where the prime denotes transposition and where Q and R are constant diagonal matrices defined as follows:

$$Q = \begin{bmatrix} Q_1 & 0 & 0 & 0 \\ 0 & Q_2 & 0 & 0 \\ \vdots & \vdots & \ddots & \vdots \\ 0 & 0 & 0 & Q_N \end{bmatrix} \ and\ R = \begin{bmatrix} R_1 & 0 & 0 & 0 \\ 0 & R_2 & 0 & 0 \\ \vdots & \vdots & \ddots & \vdots \\ 0 & 0 & 0 & R_N \end{bmatrix}$$

where $Q_i \epsilon R^{n\times n}$ and $Q_N \epsilon R^{n1\times n1}$ are positive semi-definite matrices which are used to penalize the deviation of states from zero and $R_i \epsilon R^{m\times m}$ and $R_N \epsilon R^{m1\times m1}$ are positive definite matrices which are used to penalize the control effort used to drive the states of the systems to zero.

The control which minimizes J for any set of initial conditions $X(0)$ is given by

$$U = -R^{-1}B'\widehat{K}X$$

where $\widehat{K}$ is a real symmetric positive definite constant matrix which satisfies the non-linear matrix algebraic equation

$$-\widehat{K}A - A'\widehat{K} + \widehat{K}BR^{-1}B'\widehat{K} - Q = 0$$

The controller developed above can be used to regulate the velocity and distance deviations between the follower and the leader and help in bringing down the time and distance headway for very close following.

For using this controller for GCDC simulations, we have estimated a first order point-mass model of Sommerville-Hatipoglu's complex car model. The model is as given below:

$$\dot{V} = -0.3729V + 0.3719u$$

This model is used for calculation of the controller feedback gain parameters and then the controller is implemented on the complex car model along with the FSM developed in Chapter 3. Before that, let us formulate the optimization problem for the case of GCDC competition.

Now, consider N vehicles moving in a straight line as shown in fig. 19.

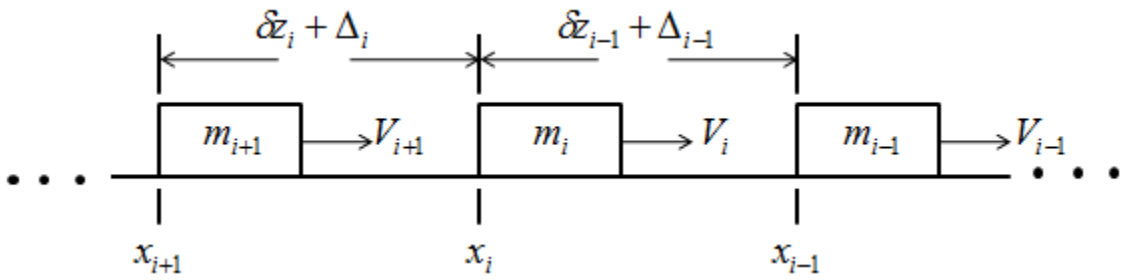

Figure 21 Vehicles moving in a convoy

where $m_i =$ mass of the ith vehicle (assumed to be constant)

$V_i =$ velocity of the ith vehicle at time t

$x_i =$ position of the ith vehicle at time t

$u_i =$ force applied to the ith vehicle at time t

$\delta z_i =$ variables used to denote deviation from the desired position

$\Delta_i =$ desired deviation between the ith and $(i+1)$st vehicle.

Here we are going to deal with the perturbation systems around desired string velocityV_{ref}, desired separation Δ_i and a constant force u_{i_0} required to overcome the drag force acting on the ith vehicle. The perturbation variables are as defined below:

$$\delta V_i = V_i - V_{ref}, \qquad for\ i = 1,2, \dots, N$$

$$\delta z_i = x_i - x_{i+1} - \Delta_i, \qquad for\ i = 1,2, \dots, N-1$$

$$\delta u_i = u_i - u_{i_0}, \qquad for\ i = 1,2, \dots, N.$$

For details of the derivation of perturbation system given above refer [9].

From the point-mass model equation and the above perturbation equations, the overall perturbation system of each vehicle is as given below:

$$\delta \dot{V}_i = -0.3729\, \delta V_i + 0.3719\, \delta u_i, \qquad for\ i = 1,2, \dots, N$$

$$\delta \dot{z}_i = \delta V_i - \delta V_{i+1}, \qquad for\ i = 1,2, \dots, N-1.$$

Thus the state-space model of the above perturbation system is as given below:

$$\begin{bmatrix} \delta \dot{V}_i \\ \delta \dot{z}_i \end{bmatrix} = \begin{bmatrix} -3.729 & 0 \\ 1 & 0 \end{bmatrix} \begin{bmatrix} \delta V_i \\ \delta z_i \end{bmatrix} + \begin{bmatrix} 0.3719 \\ 0 \end{bmatrix} \delta u_i, \qquad for\ i = 1,2, \dots, N-1$$

And $$\delta \dot{V}_i = -0.3729\, \delta V_i + 0.3719\, \delta u_i, \qquad for\ i = N$$

Now, the GCDC scenarios have been simulated with a set of 6 vehicles. As explained in chapter 1, there are going to be two convoys starting one behind each other but each from behind a traffic light. Three vehicles have been used in each convoy. Vehicle 1, 2 and 3 are part of convoy 1 and vehicles 4, 5 and 6 are part of convoy 2. Convoy 1 is ahead of convoy 2. Same setup has been used here which is going to be used in the competition. The urban scenario is followed by the highway scenario in

which the lead/ phantom vehicle introduces some disturbances similar to the ones found on actual highways.

Here, the two convoys are taken to be 465 m apart initially. A trigger line is assumed to be located at 400 m. So, as soon as vehicle 4 crosses 400 m mark, convoy 1 is triggered and set into motion with the lead/phantom vehicle having a cruise speed of 25 mph for the urban scenario. After the two convoys merge smoothly, they travel at the lead cars speed till the last vehicle passes the 1500 m mark. As soon as the last vehicle crosses the mark, the urban scenario ends and the highway scenario starts and the convoy starts to move at 45 mph for the highway scenario. The lead/phantom vehicle introduces a disturbance into the convoy. We have added a sinusoidal disturbance with amplitude of $2mph$ and a frequency of $1rad/s$. The convoy needs to exhibit string stability while maintaining least possible following distance and the least possible headway time.

The simulation results are provided for vehicles with different masses. Figures 22, 25 and 28 show the velocities of all the vehicles. Figures 23, 26 and 29 show the relative velocities of the current vehicle and its follower. Figures 24, 27 and 30 show the inter-vehicular distance between the current vehicle and its follower.

(i) Case 1 – $M_1 = M_2 = M_3 = M_4 = M_5 = M_6$:

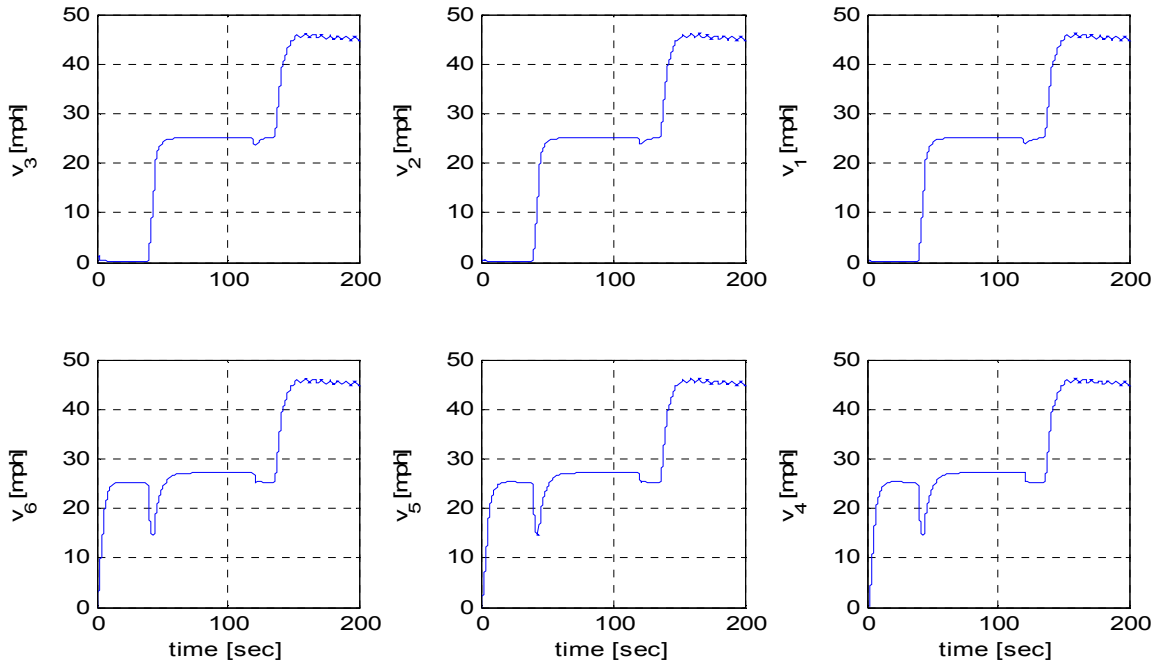

Figure 22 Velocities of vehicles

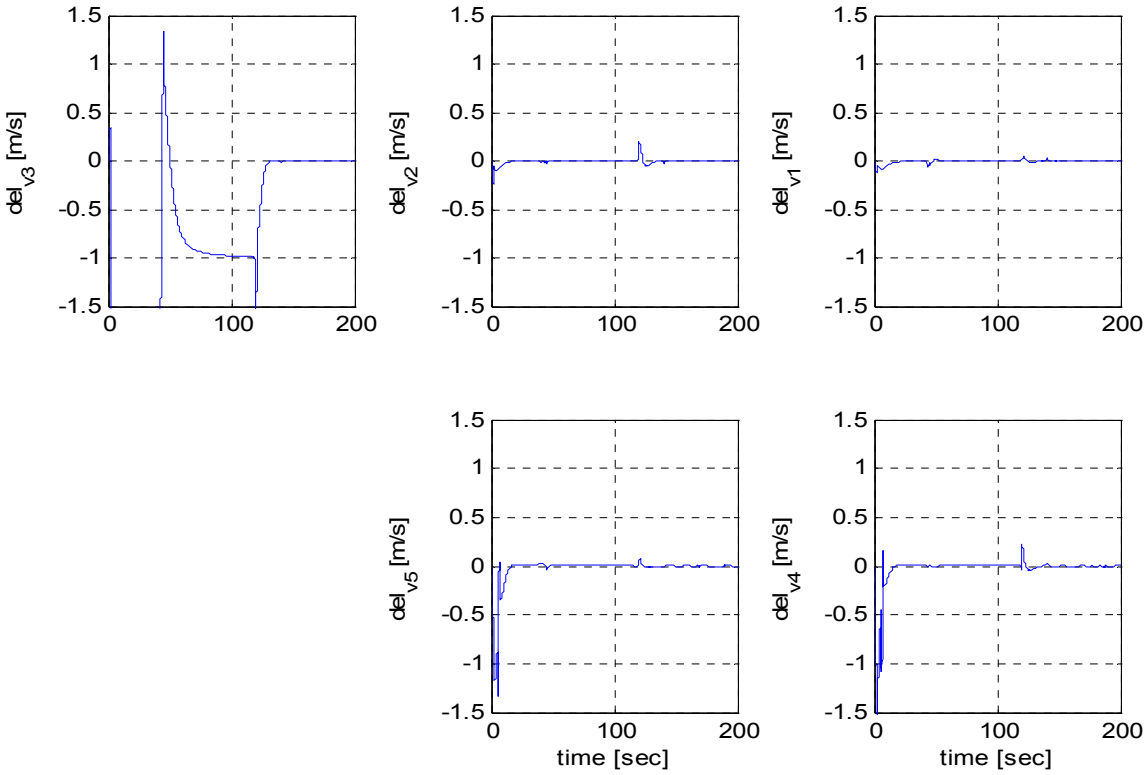

Figure 23 Relative Velocity between the vehicles

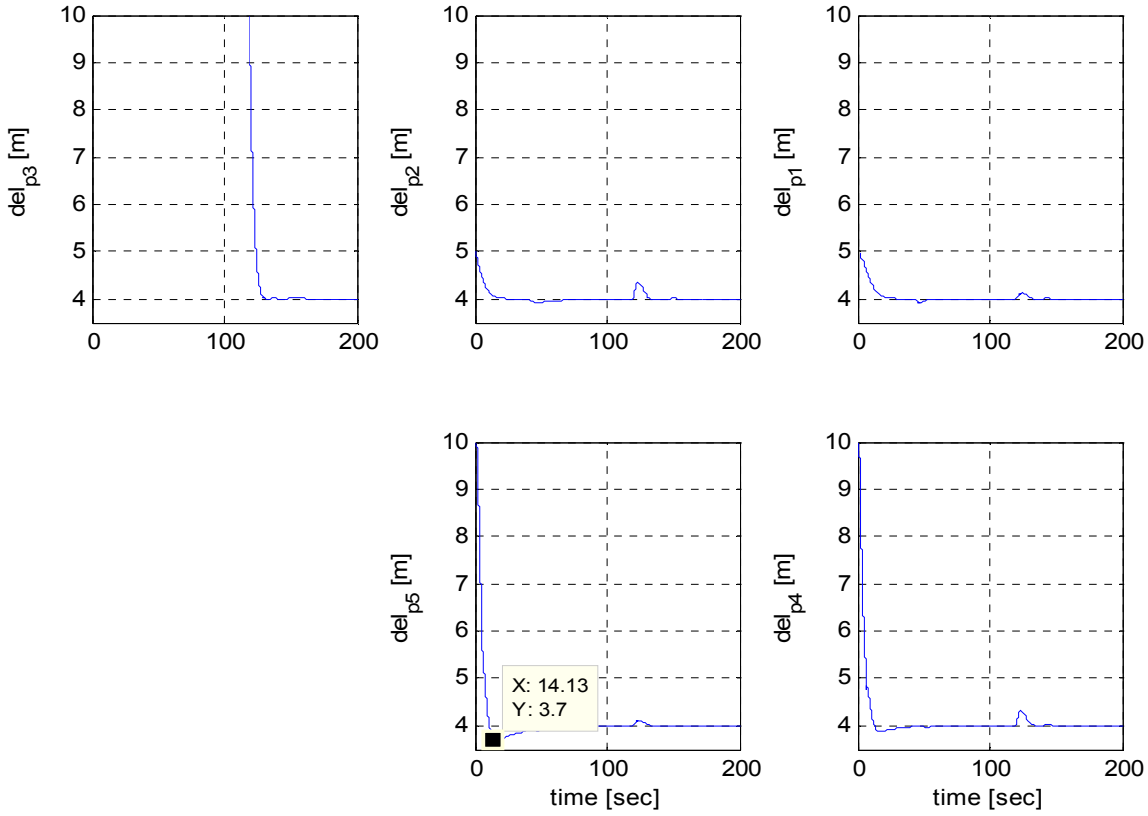

Figure 24 Relative Distance between vehicles

(ii) Case 2 - $M_1 > M_2 > M_3 > M_4 > M_5 > M_6$:

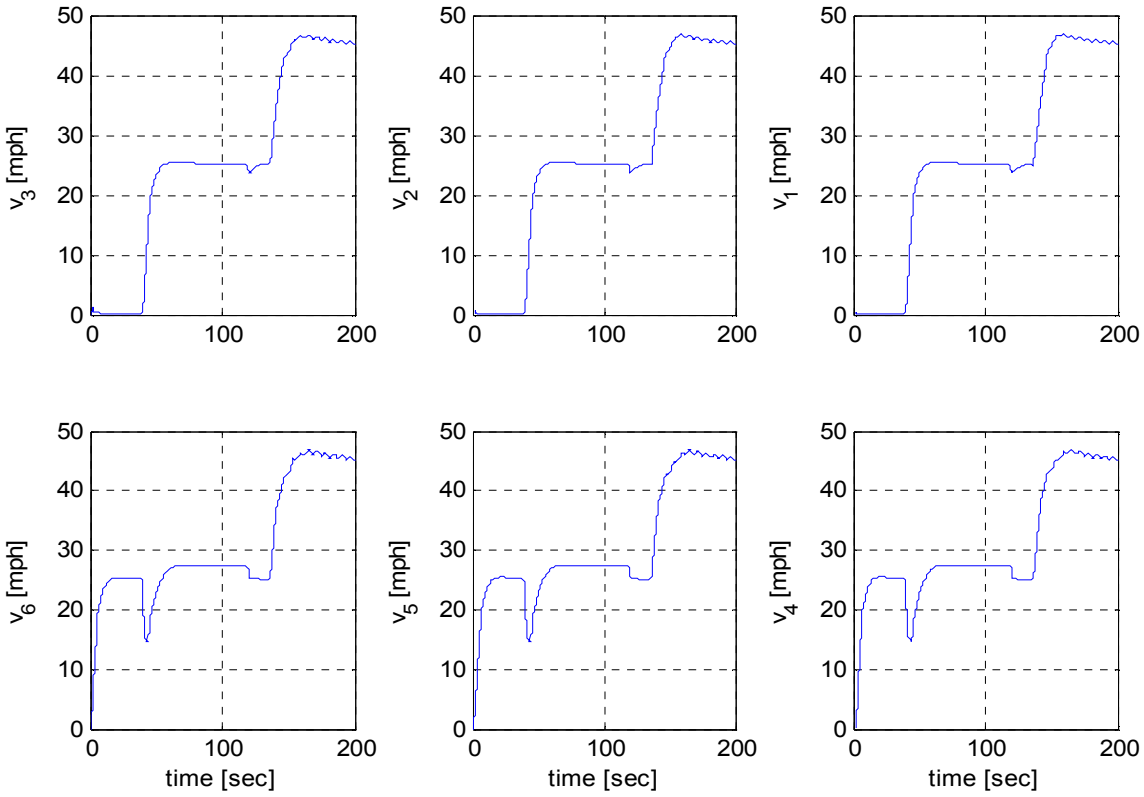

Figure 25 Velocities of vehicles

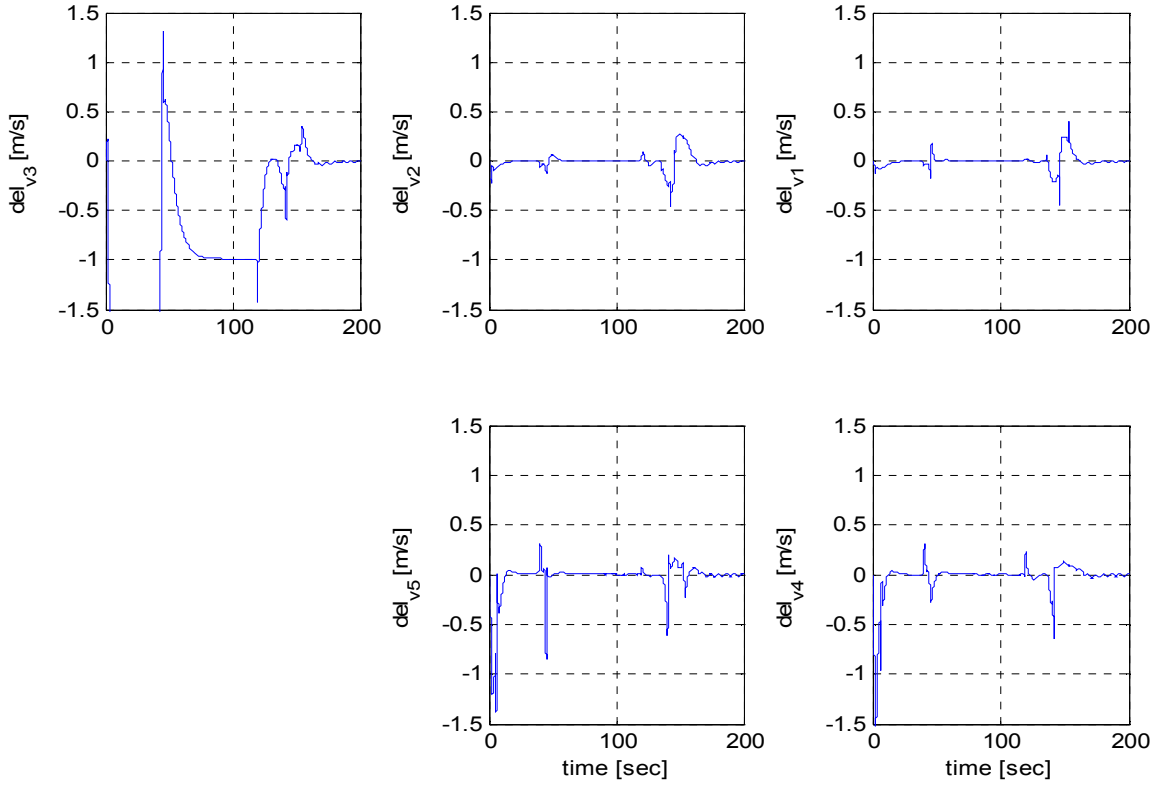

Figure 26 Relative Velocity between the vehicles

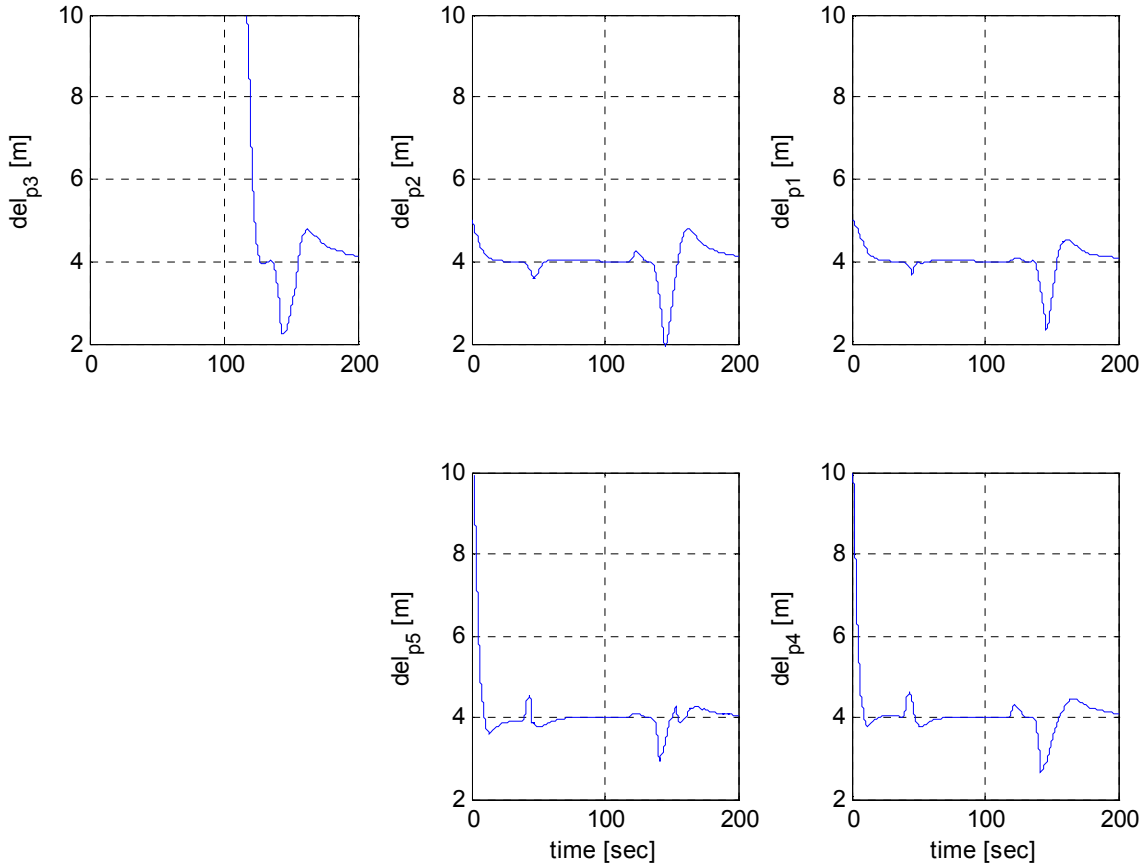

Figure 27 Relative Distance between vehicles

(iii) Case 3 - $M_1 < M_2 < M_3 < M_4 < M_5 < M_6$:

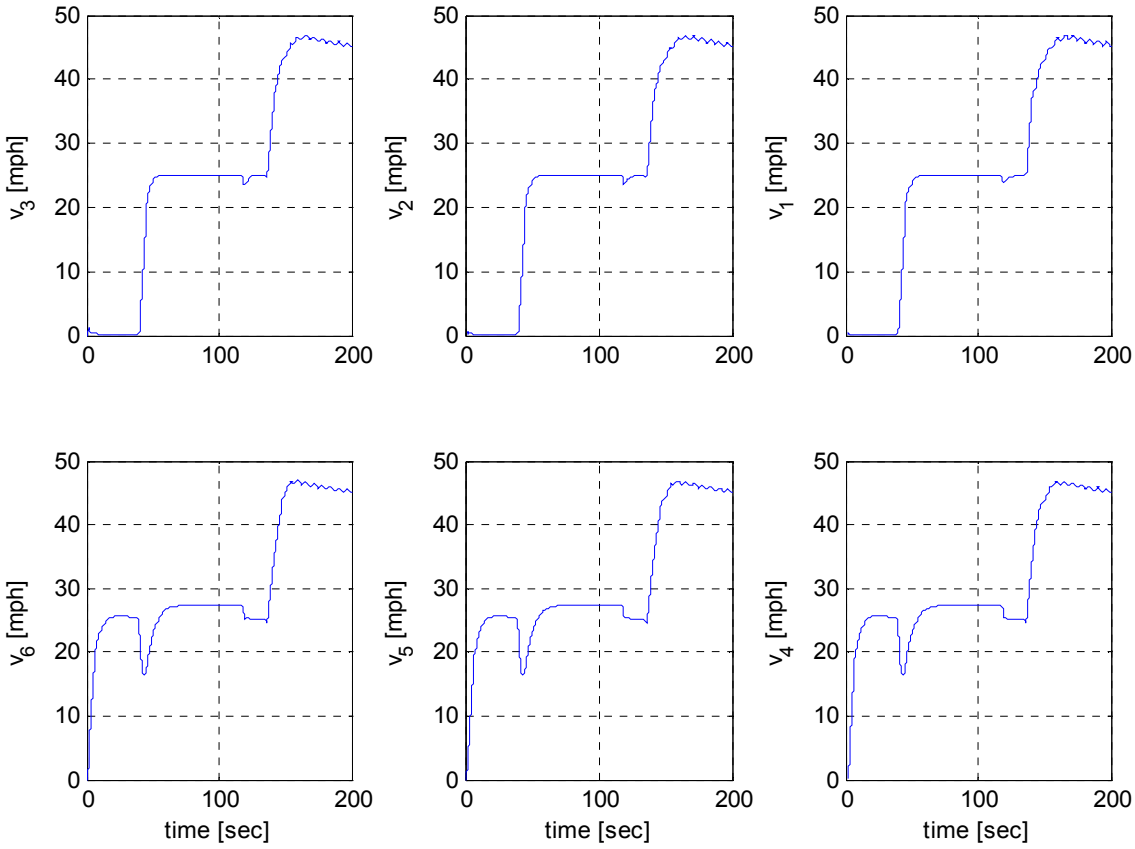

Figure 28 Velocities of vehicles

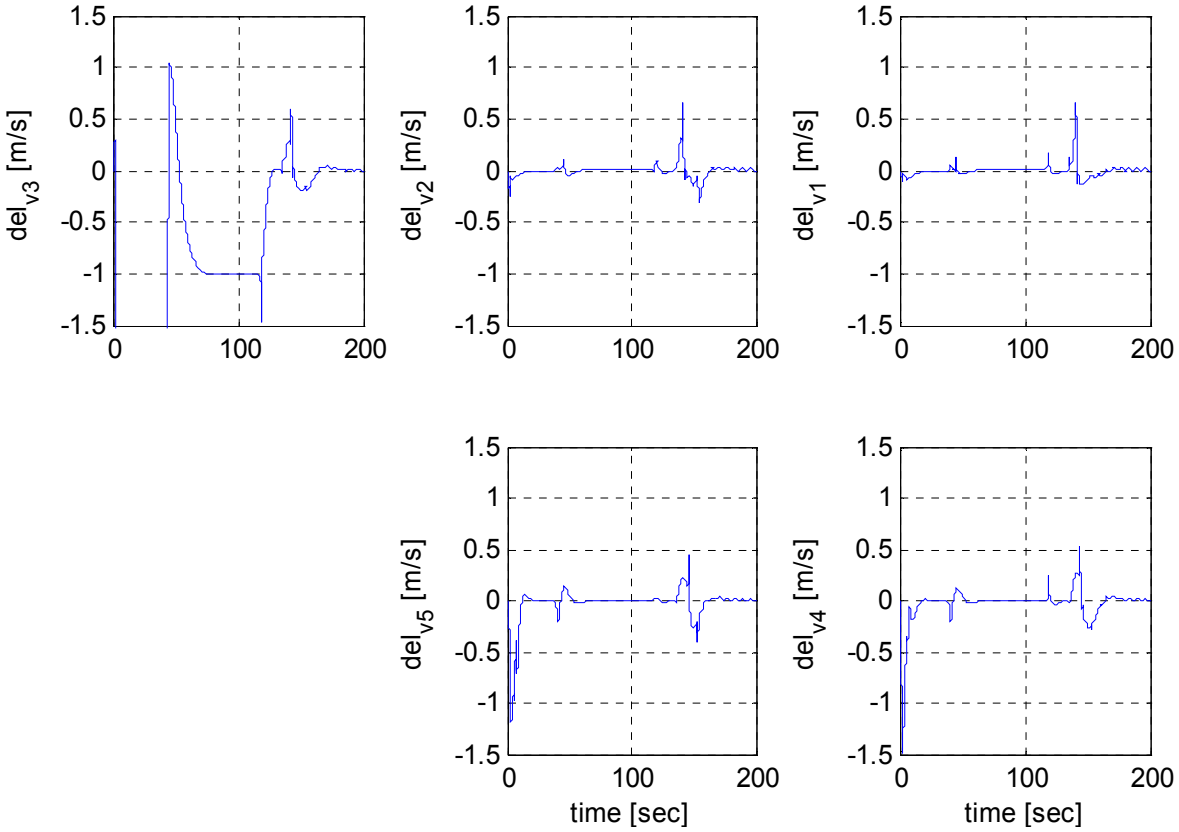

Figure 29 Relative Velocity between the vehicles

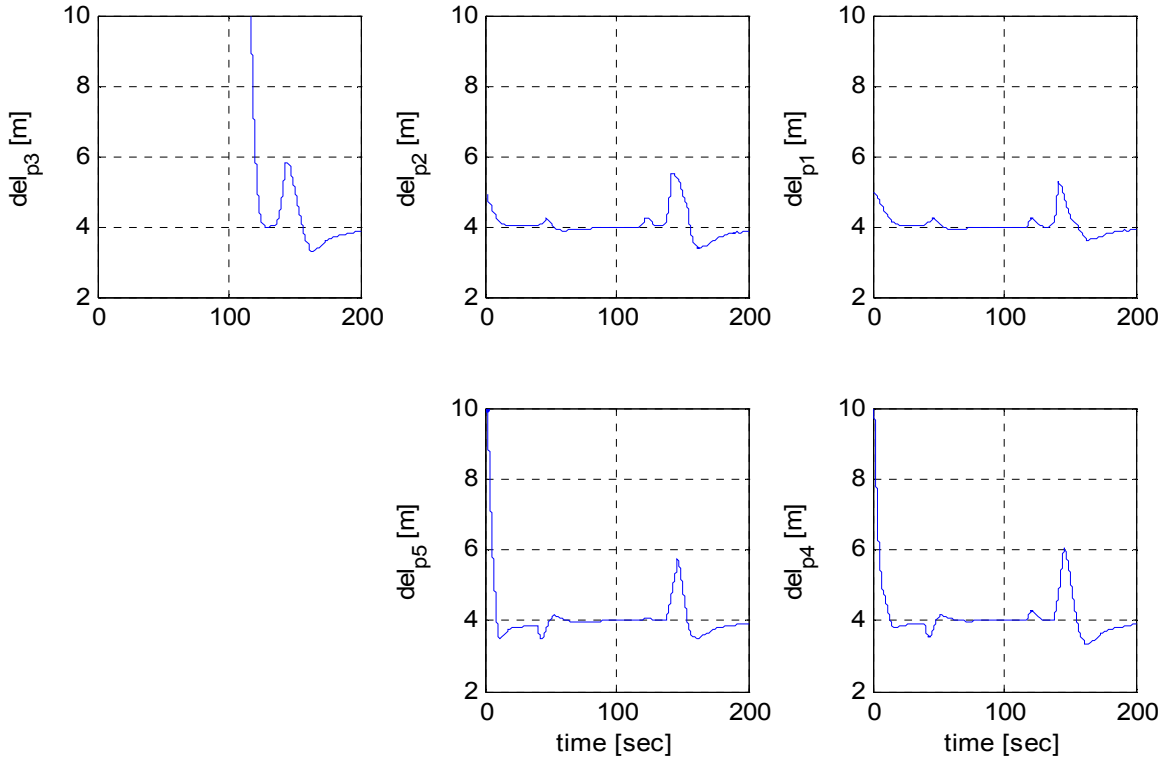

Figure 30 Relative Distance between vehicles

The vehicle masses for case 1 are all 130.578 slugs. For case 2, we have taken vehicle 6 to be 130.578 slugs and each preceding vehicle 20 slugs heavier than the following vehicle. For case 3, we have taken vehicle 1 to be 130.578 slugs and each following vehicle 20 slugs heavier than its leader. From figures 22, 25 and 28 we can see that convoy 2 merges smoothly behind convoy 1between 30 sec and 40 sec, where we see a dip in the velocities of vehicles 4, 5 and 6. Also, the entire convoy maintains string stability as the velocity disturbance is not amplified by any of the vehicles after the highway scenario starts. Comparing figures 23, 26 and 29 we see that the excursion of the inter-vehicular velocities is almost zero for case 1 when all the vehicles have the same mass which causes the inter-vehicular distance to remain almost constant at 4

m. The excursion in inter-vehicular velocity slightly increases in the negative direction for case 2 where the masses of the vehicles decrease successively leading to a negative excursion in following distance. This is obvious as lighter vehicles are following the heavier ones and hence they respond than their preceding vehicle when there is a sudden increase in the reference velocity. For case 3, the excursion in the inter-vehicular velocities is slightly on the positive side as the heavier vehicles are following the lighter ones and hence they respond slightly sluggishly than the preceding vehicle. Hence we see a small positive excursion in following distance.

4.2.LQR-based Sequential State-feedback Controller

Ozguner and Perkins 1977 [10] considered the problem of optimum control of multilevel composite systems and designed regulators for linear multilevel composite systems with local quadratic cost functions. A brief introduction of the same is given in this section.

Consider a multilevel large-scale composite (LSC) system which is modeled as an interconnection of subsystems $s_i, i = 1, \dots, N$ as shown below:

$$s_1 : \dot{x}_1 = A_1 x_1 + B_1 u_1$$

$$y_1 = C_1 x_1$$

where $x_1 \in R^{n1}$, $u_1 \in R^{m1}$, $A_1 \in R^{n1 \times n1}$ and $B_1 \in R^{n1 \times m1}$.

$$s_i : \dot{x}_i = A_i x_i + \sum_{j=1}^{i} B_j^i u_j^i$$

$$y_i = C_i x_i, \quad i = 2, \dots, N$$

where $$u_j^i = h_{ji} y^j, \ j < i$$

and $x_i \in R^n$, $u_i \in R^m$, $A_i \in R^{n \times n}$ and $B_i \in R^{n \times m}$. Here $n \neq n1$.

Now, the cost function associated with each subsystem is as given below:

$$J_i = \int_0^\infty x_i^T Q_{ii} x_i + u_i^{iT} R_{ii} u_i^i) dt, \quad i = 1, \dots, m$$

where $Q_{ii}^T = Q_{ii} \geq 0, R_{ii}^T = R_{ii} > 0.$

Now, a solution to the sequential steady-state, state regulator problem for the multilevel LSC system mentioned above with cost function J_i, where each constituent is locally stabilizable and the pairs (D_i, A_i) are detectable (where $Q_{ii} = D_i^T D_i$), exists, is unique and is given by

$$u_i^i = -R_{ii}^{-1} B_i^{iT} \left(\sum_{j=1}^{i} P_{ij} x^j \right)$$

where P_{ii} is obtained as a solution of a local linear state regulator (LLSR) problem whose solution is found from the algebraic Riccati equation

$$-P_{ii}^i A_i - A_i^T P_{ii}^i - Q_{ii} + P_{ii}^i B_i^i R_{ii}^{-1} B_i^{iT} P_{ii}^i = 0$$

and $P_{i,i-1}$ from the linear matrix equation

$$P_{i,i-1} A_{i-1}^* + A_i^{*T} P_{i,i-1} = -P_{ii} \left(B_{i-1}^i h_{i,i+1} C^{i-1} \right)$$

and P_{ij} for $j < i - 1$, for the linear matrix equations

$$P_{ij} A_j^* + A_i^{*T} P_{ij} = -\left[\sum_{k=j+1}^{i-1} P_{ik} \left(B_j^k h_{jk} C_j + B_k^k K_j^k \right) \right] - P_{ii} B_j^i C_j$$

The controller developed above again can be used to regulate the velocity and distance deviations between the follower and the leader and help in bringing down the time and distance headway for very close following.

The same first-order estimated model of the complex car model given in section 4.1. is used for the calculation of the feedback gains mentioned above and then the

controller is implemented on the complex car model along with the FSM developed in Chapter 3. Before that, let us formulate the optimization problem for the case of GCDC competition.

Now, consider N vehicles moving in a straight line as shown in Figure 31.

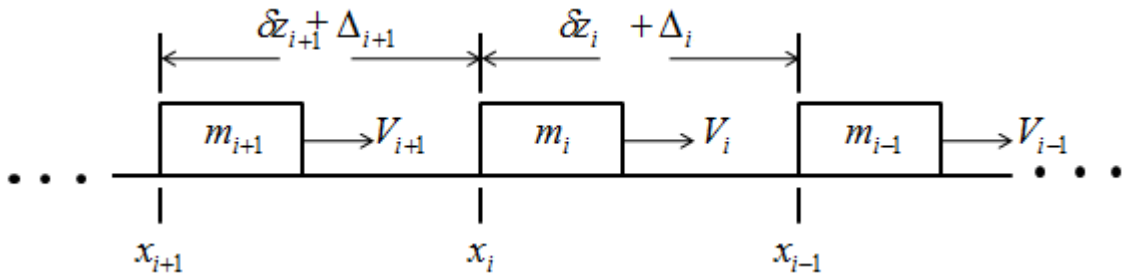

Figure 31 Vehicles moving in a convoy

The variable definitions remain the same as mentioned in section 4.1.

Here we are going to deal with the perturbation systems around desired string velocityV_{ref}, desired separation Δ_i and a constant force u_{i_0} required to overcome the drag force acting on the ith vehicle. The perturbation variables are as defined below:

$$\delta V_i = V_i - V_{ref}, \qquad for\ i = 1,2, \dots, N$$

$$\delta z_i = x_{i-1} - x_i - \Delta_i, \qquad for\ i = 2, \dots, N$$

$$\delta u_i = u_i - u_{i_0}, \qquad for\ i = 1,2, \dots, N.$$

For details of the derivation of the perturbation system given above refer [10].

From the point-mass model equation and the above perturbation equations, the overall perturbation system of each vehicle is as given below:

$$\delta \dot{V}_i = -0.3729\, \delta V_i + 0.3719\, \delta u_i, \qquad for\ i = 1,2, \dots, N$$

$$\delta \dot{z}_i = \delta V_{i-1} - \delta V_i, \qquad for\ i = 2, \dots, N.$$

Thus the state-space model of the above perturbation system is as given below:

$$\delta \dot{V}_i = -0.3729\, \delta V_i + 0.3719\, \delta u_i, \qquad for\ i = 1$$

And $$\begin{bmatrix} \delta \dot{V}_i \\ \delta \dot{z}_i \end{bmatrix} = \begin{bmatrix} -3.729 & 0 \\ -1 & 0 \end{bmatrix} \begin{bmatrix} \delta V_i \\ \delta z_i \end{bmatrix} + \begin{bmatrix} 0.3719 \\ 0 \end{bmatrix} \delta u_i \quad for\ i = 2, \dots, N.$$

The GCDC scenarios have been simulated with a set of 6 vehicles for this controller. In this case, the first state used for feedback is the velocity deviation of the vehicle from the reference velocity and the second state is its distance from the preceding vehicle. This is slightly different from the controller used in previous section in a way that the previous controller used the first state same as this controller but the second state was the distance of the vehicle from its following vehicle rather than its preceding vehicle. Simulation results are provided for the same three cases as in section 4.1.

(i) Case 1 – $M_1 = M_2 = M_3 = M_4 = M_5 = M_6$:

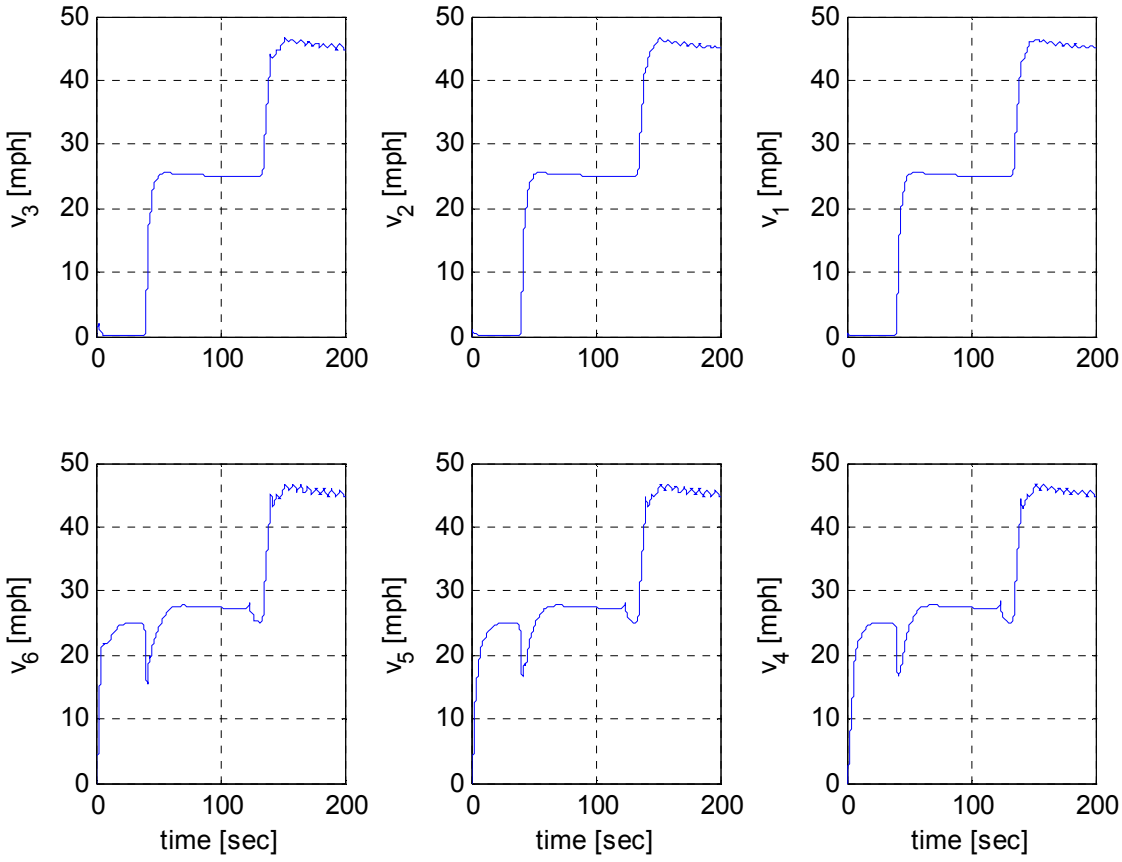

Figure 32 Velocities of vehicles

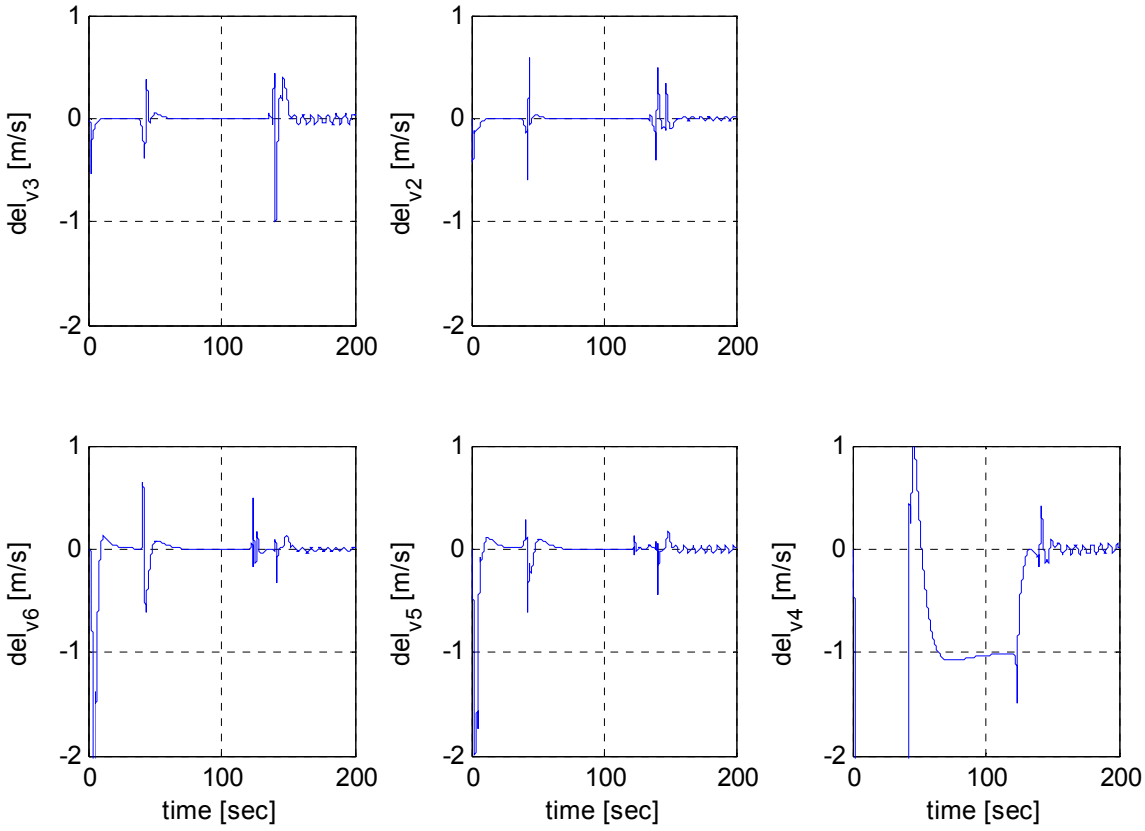

Figure 33 Relative Velocity between the vehicles

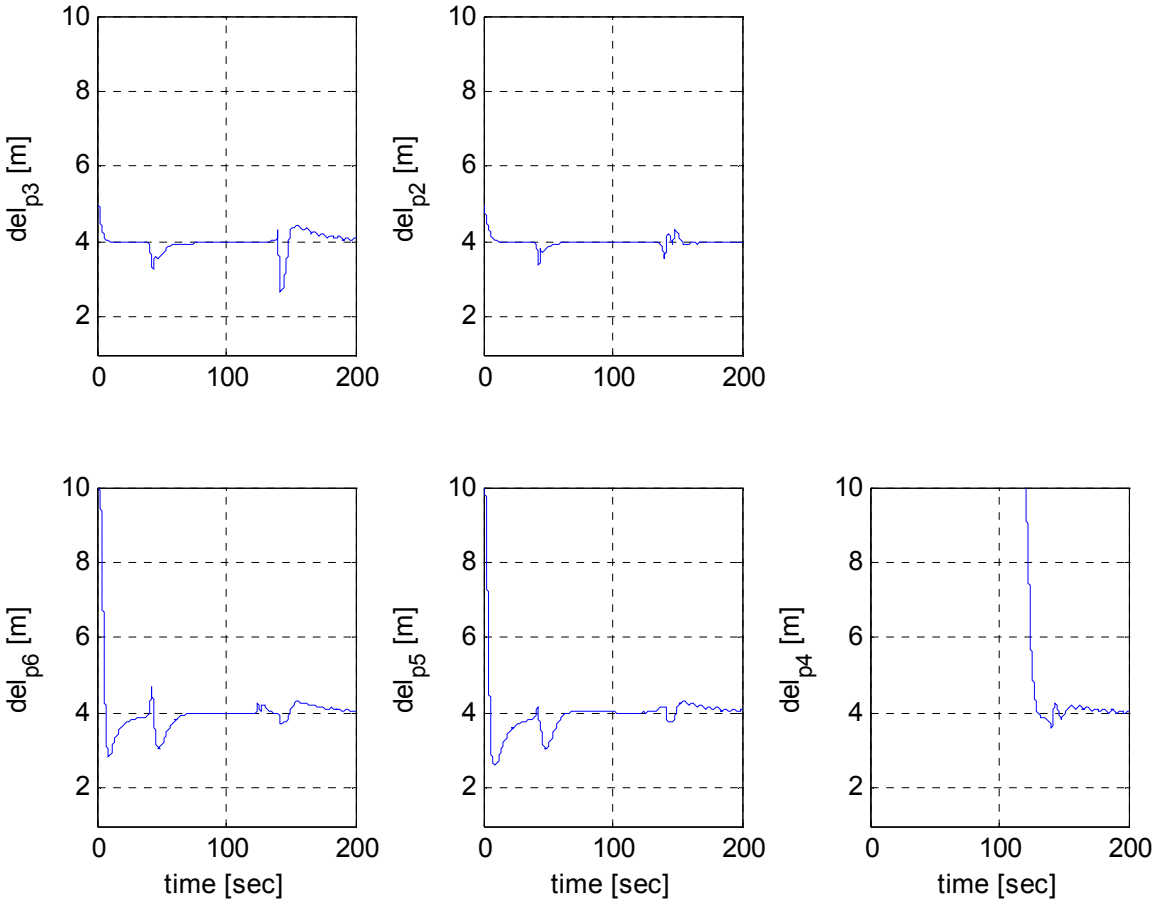

Figure 34 Relative Distance between vehicles

(ii) Case 2 - $M_1 > M_2 > M_3 > M_4 > M_5 > M_6$:

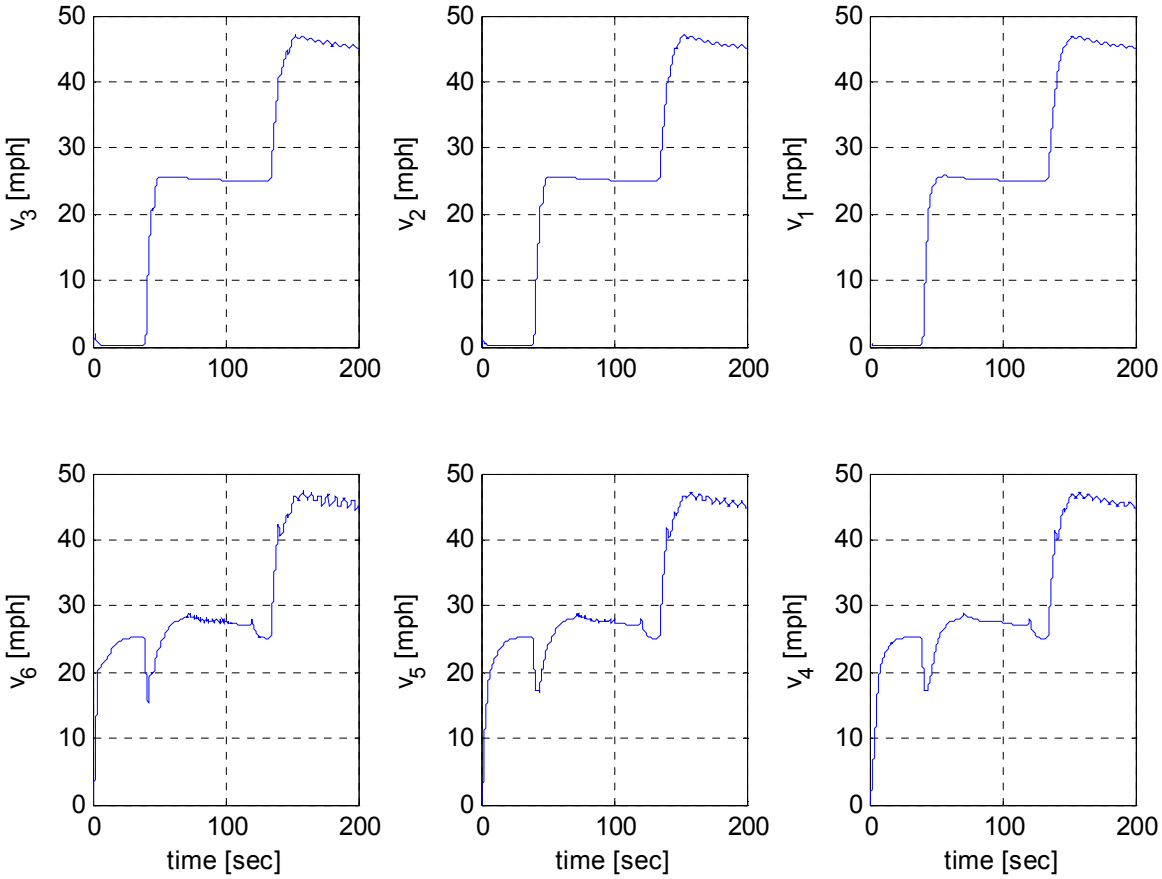

Figure 35 Velocities of vehicles

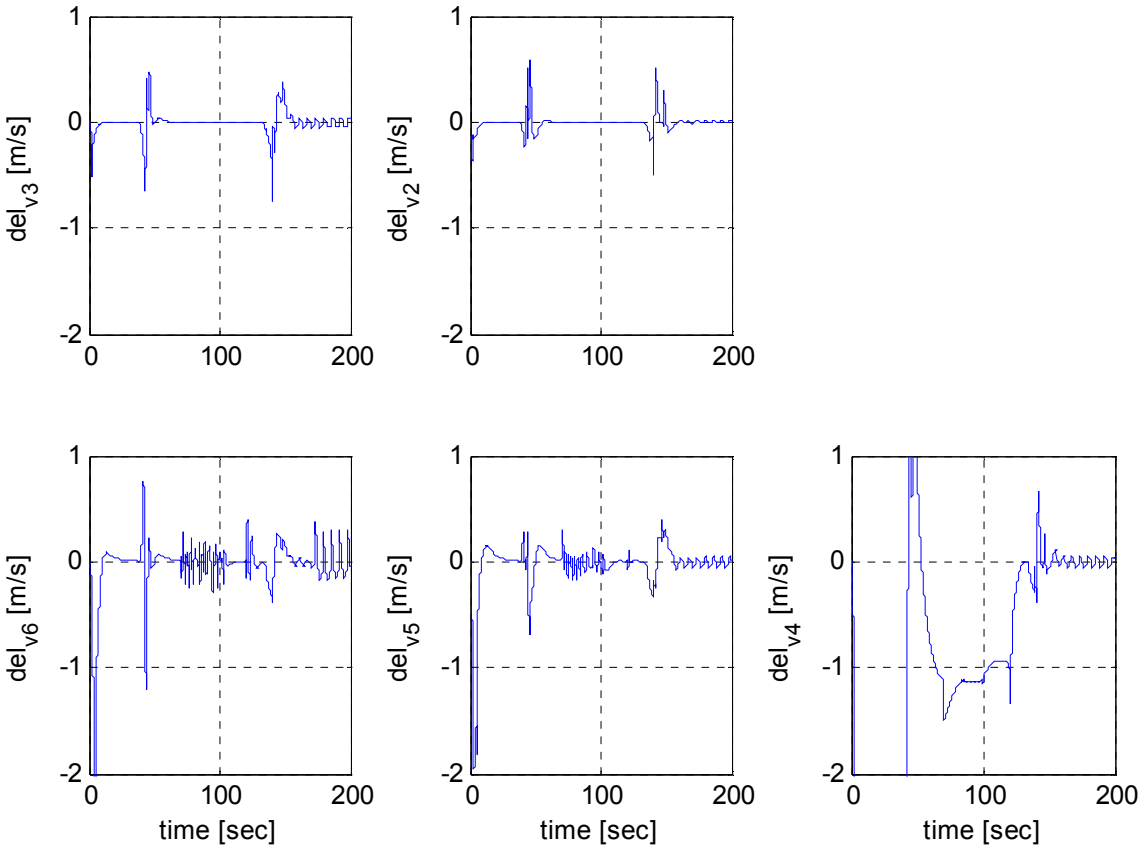

Figure 36 Relative Velocity between the vehicles

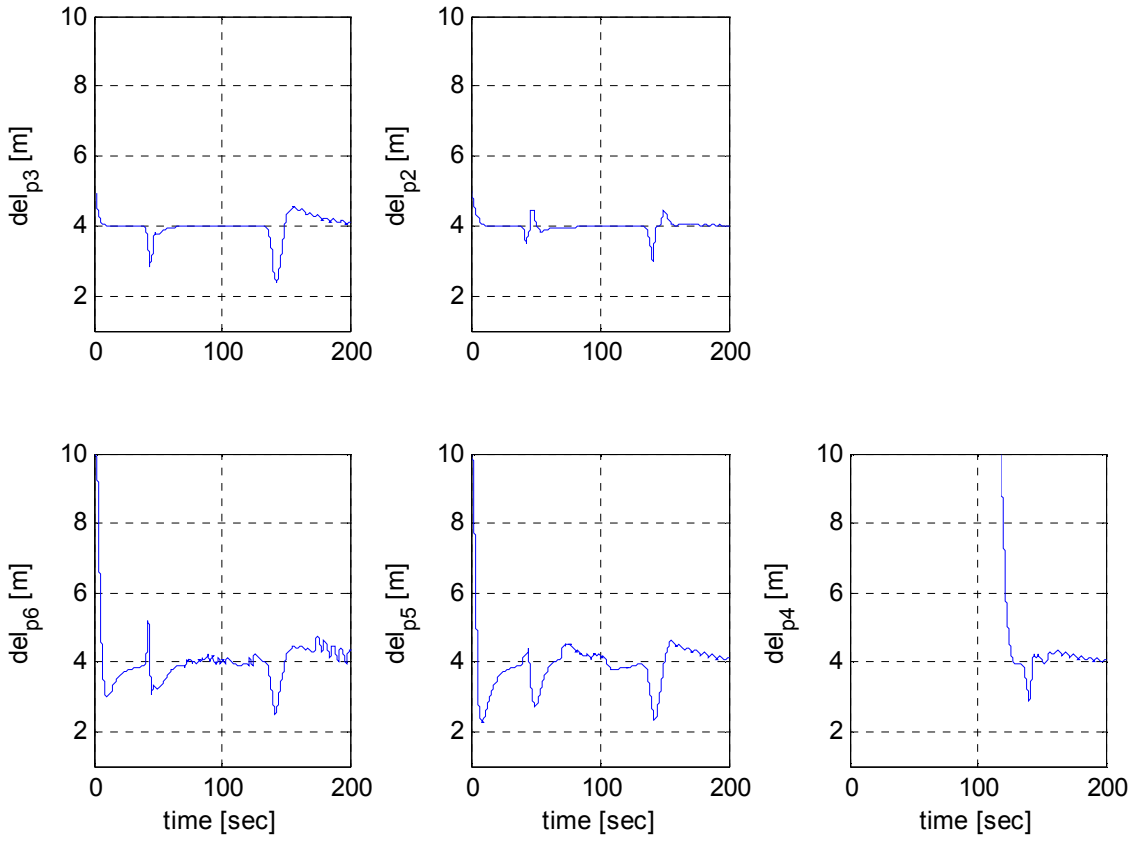

Figure 37 Relative Distance between vehicles

(iii) Case 3 - $M_1 < M_2 < M_3 < M_4 < M_5 < M_6$:

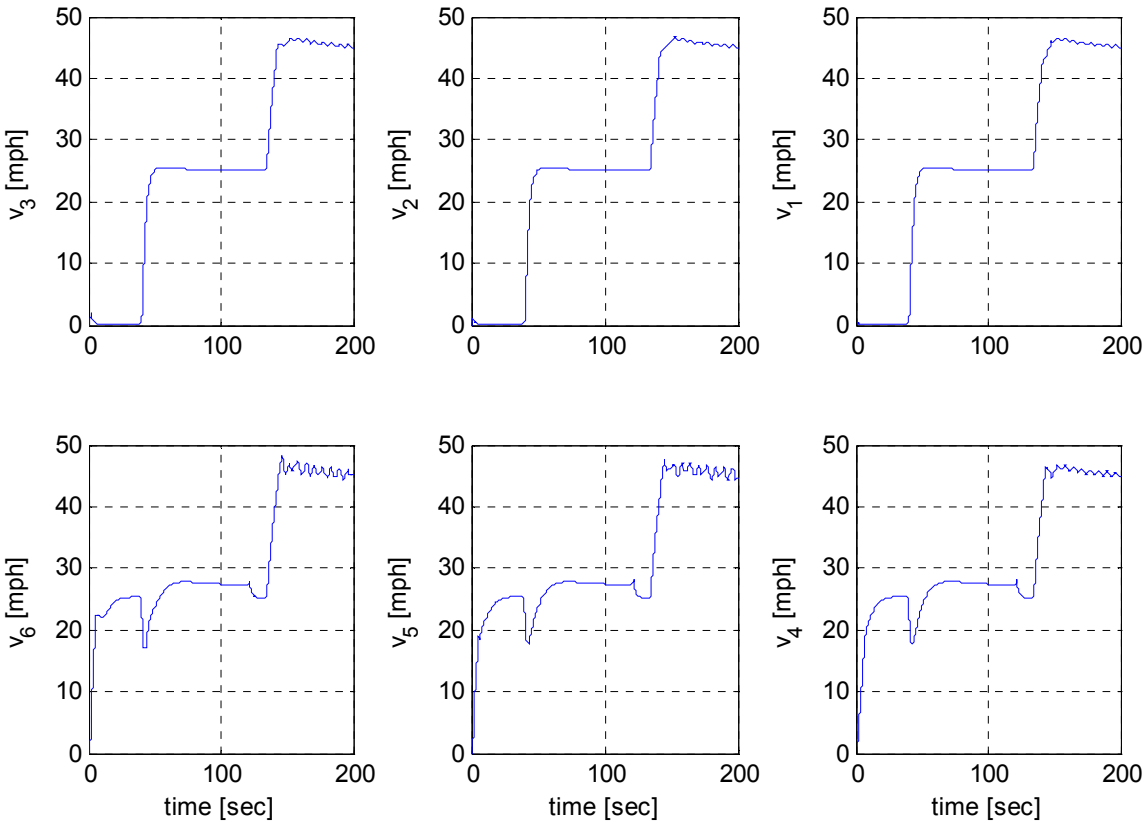

Figure 38 Velocities of vehicles

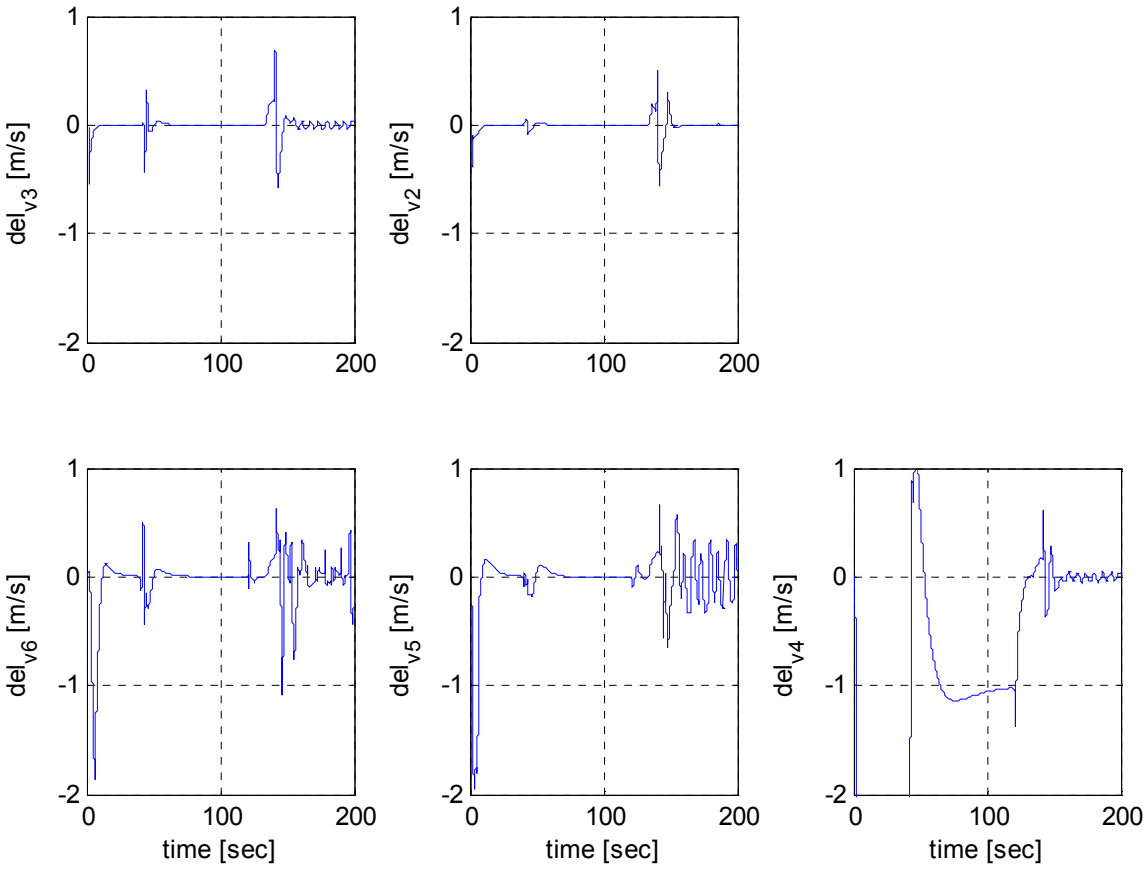

Figure 39 Relative Velocity between the vehicles

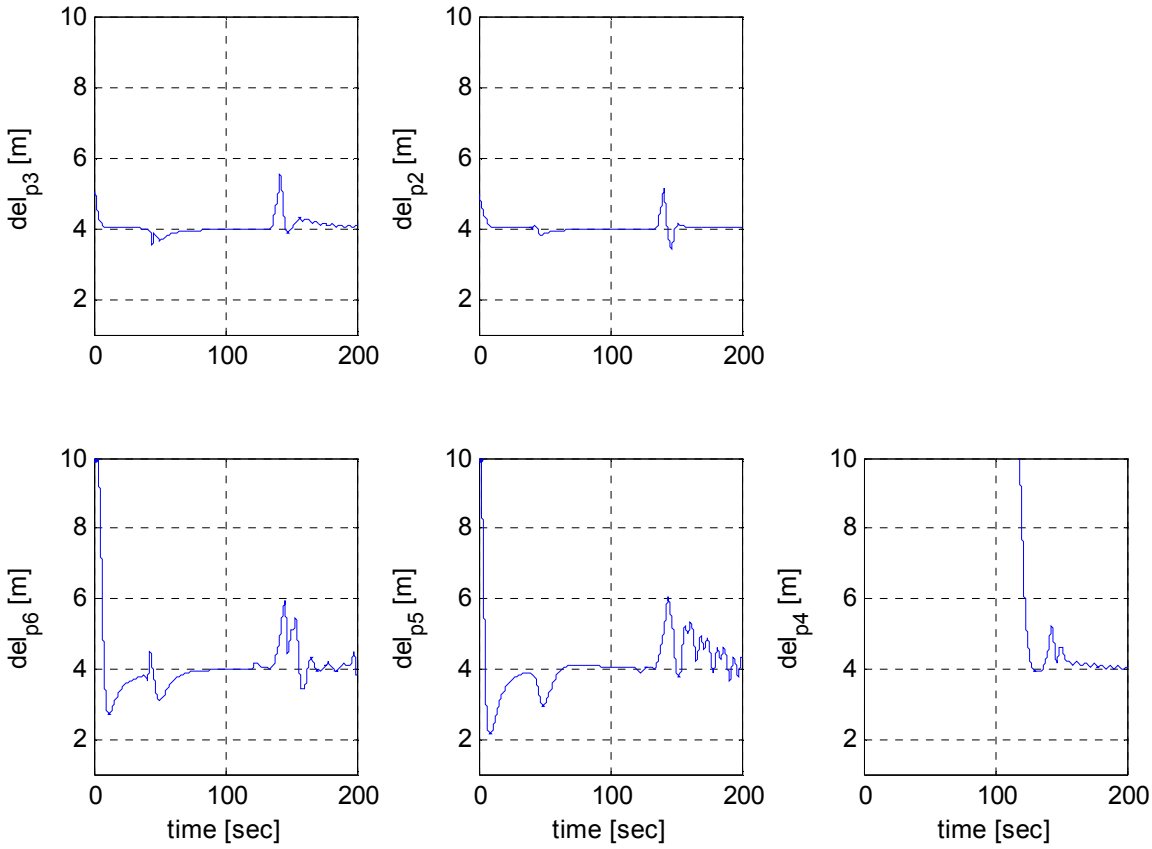

Figure 40 Relative Distance between vehicles

The vehicle masses used for case 1 and 2 are the same as the ones used for the simulations in section 4.1. For case 3 we have used increments of 10 slugs between each vehicle and its follower as this controller produces a positive excursion of 4 m for vehicles being 20 slugs heavier than their preceding vehicles. From figures 32, 35 and 38 we can see that convoy 2 merges relatively smoothly behind convoy 1between 30 sec and 40 sec, where we see a dip in the velocities of vehicles 4, 5 and 6. Also, the entire convoy maintains string stability as the velocity disturbance is not amplified by any of the vehicles after the highway scenario starts. Comparing the simulation results for the two controllers we find that the LQR based full-state feedback produces better regulation of the following vehicles than the LQR based sequential state feedback controller. This is

because excursion of the states of any vehicle in the convoy affect the control effort fed back to each vehicle for the full-state feedback controller, whereas for the sequential state feedback controller assumes a priori that no useful information can be supplied by the following vehicles [10].

CHAPTER 5 CONCLUSIONS

5.1.Summary of Work

The purpose of this thesis was to present the results of a simulation study of using two different types of car following controllers working along with a FSM on a complex car model. The above Master Controller was developed with a vision of implementing it on a real car for the GCDC Competition which is going to be held next year.

Chapter 2 provided an overview of different types of car models that were used in previous studies. We saw that the point-mass model was computationally simple and less expensive but did not incorporate any non-linearities which are inherent in a vehicle. Takaski-Fenton modeled a 1969 Plymoth Sedan which incorporated the electrohydraulic actuator/engine-drivetrain combustion, non-linear frictional forces impeding the motion of the vehicle and wheel slip. This model was still not adequate as the torque convertor dynamics were ignored as well as the vehicle did not account for any braking. The model developed by Martin Somerville of a 1992 Honda Accord took care of most of the system dynamics found in a modern vehicle like the engine dynamics, torque convertor dynamics, transmission dynamics, vehicle dynamics, throttle as well as the brake actuators making it the only choice for such a simulation study.

The Longitudinal FSM used on the car model for dealing with different states during a leader-follower approach and follow maneuver is discussed in chapter 3. A detailed description of all the states of the FSM is provided. The different states used for our simulation study were – cruise, approach, follow, emergency brakes and hard braking.

In chapter 4, we have mentioned about two close following controllers and implemented them on a first order vehicle model which we have estimated from Sommerville-Hatipoglu's complex car model along with the Longitudinal FSM for the two GCDC scenarios.

5.2.Conclusion

We have tested the two LQR based close following controllers along with the Longitudinal FSM on a complex car model. Both the controllers give promising results and hence can be implemented in future to reduce the vehicle following distance as well as to increase the efficiency of the current road infrastructure. A comparison study showed that the LQR based full state-feedback gives better regulation than the LQR based sequential state-feedback. But the latter is practically feasible due to the following reasons:

(i) With single cost function for a system with N vehicles $\frac{1}{2}[(2m+1)(2m+2)]$ coupled equations have to be solved.

(ii) The total number of communication links required between all the vehicles in the convoy reduces approximately by 50% as compared to the LQR based full state-feedback controller.

(iii) When a $(N+1)^{st}$ vehicle augments the convoy, feedback gains for N vehicles is not required to be calculated. Only the feedback gains for the $(N+1)^{st}$ need to be calculated making the controller a "distributed controller" rather than a "centralized controller" like the full state-feedback controller. This makes it extremely practical.

5.3.Future Directions

We have implemented the longitudinal controllers on a complex vehicle model. But these controllers need to be tested on real cars and in a convoy type situation.

We have assumed that we have a lossless and a delay free medium of communication. In most of the real life scenarios, this is not true. A study on which type of V-2-V network to be used to minimize transmission as well as transport delays should be performed and a controller which deals with the delay in receiving information either from the sensors or sending information to the actuators should be developed. The Finite State Machine can be improved to include more states to avoid obstacles and even to stop at a red light. Lateral controllers should be developed and added to the longitudinal model to make a complete autonomous car which is able to negotiate lane change and turning maneuvers.

APPENDIX - COMPLETE LONGITUDINAL MODEL

Martin Sommerville and Cem Hatipoglu completely modeled a 1992 Honda Accord [7]. We have made a few changes to the model like, tuning the gains of the controllers and adding the integral wind-up's for the PID controllers.

6.1.Sommerville-Hatipoglu Longitudinal Model

This model is a simple longitudinal dynamics model of the vehicle which can be used for cruise control type operations. The model is as shown below:

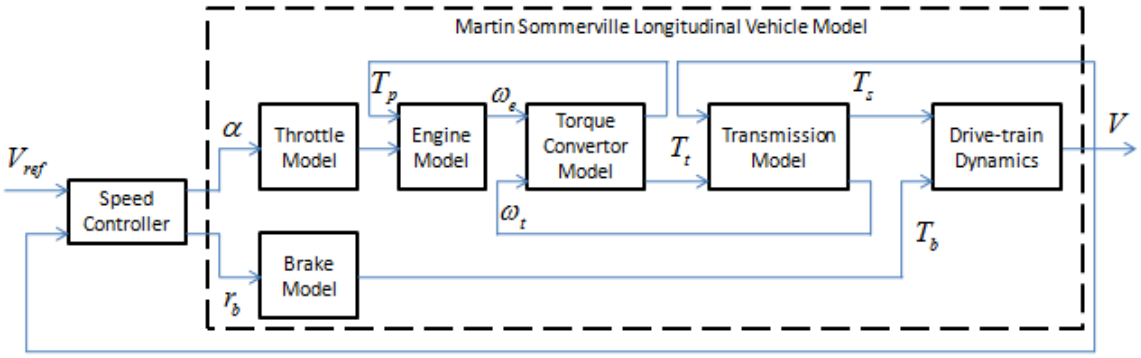

Figure 41 Longitudinal vehicle model for cruise control (C.Hatipoğlu, Ü.Özgüner and M.Sommerville, 1996)

The physical meaning of the variables is given in below:

V_{ref} = Reference speed or desired speed of the vehicle

V = Longitudinal velocity of the vehicle model

ω_e = Engine speed

ω_t = Turbine speed

T_s = Torque from transmission after final gear reduction

T_t = Turbine torque (output of torque convertor)

T_p = Pump torque (feedback from torque convertor pump)

T_b = Braking torque

α = Throttle angle

r_b = Desired braking force

Here the desired speed is fed to the speed controller and it produces the exact throttle or brake command required to regulate the speed of the vehicle and reduce the error in desired speed and vehicle speed to zero. A brief explanation of Sommerville-Hatipoglu's model is given below. Refer to [7] for more details.

The desired speed is converted in to ft/sec as the entire model works with CGS units. The model has detailed blocks of engine dynamics, torque-convertor dynamics, transmission model, drive-train dynamics, brake actuator model and brake control unit, throttle actuator model and throttle control unit and gear select unit. This model contains a master speed controller which switches the control from the throttle controller mode to the brake controller mode and vice-versa depending on the mode of operation. The mode of operation is calculated by a finite state machine which takes the desired speed, estimated speed, the throttle control output, brake control output and the previous mode as an input.

Now let us talk one-by-one about different blocks inside the vehicle model.

6.2.Vehicle Dynamics Model

The vehicle dynamics model consists of the Engine dynamics model, Torque Convertor model, Transmission model and the Drivetrain dynamics model. These blocks have been discribed below:

6.2.1. Engine Dynamics Model

The differential equation discribing the engine is as shown below:

$$\dot{\omega}_e = \frac{1}{J_e}\{T_c(\alpha + \alpha_{offset}, \omega_e) - T_a(\omega_e) - T_p(\omega_e, \omega_t)\}$$

where α = throttle angle (deg)

ω_e= engine speed (rpm)

ω_t= torque convertor turbine speed (rpm)

J_e = engine inertia (ft.lbs.sec^2)

T_c = engine engine combustion torque (ft.lbs)

T_a = engine accessory and load torque (ft.lbs)

T_p = feedback from torque convertor pump (ft.lbs)

The accessory and load torque is approximated as

$$T_a = 1.0337\ (\omega_e)^{0.2}\ \ ft.lbs$$

The engine model basically consists of a look-up table for the torque produced by the engine combustion for certan combination of throttle angle and engine speed. The torque map has been shown in Figure 42.

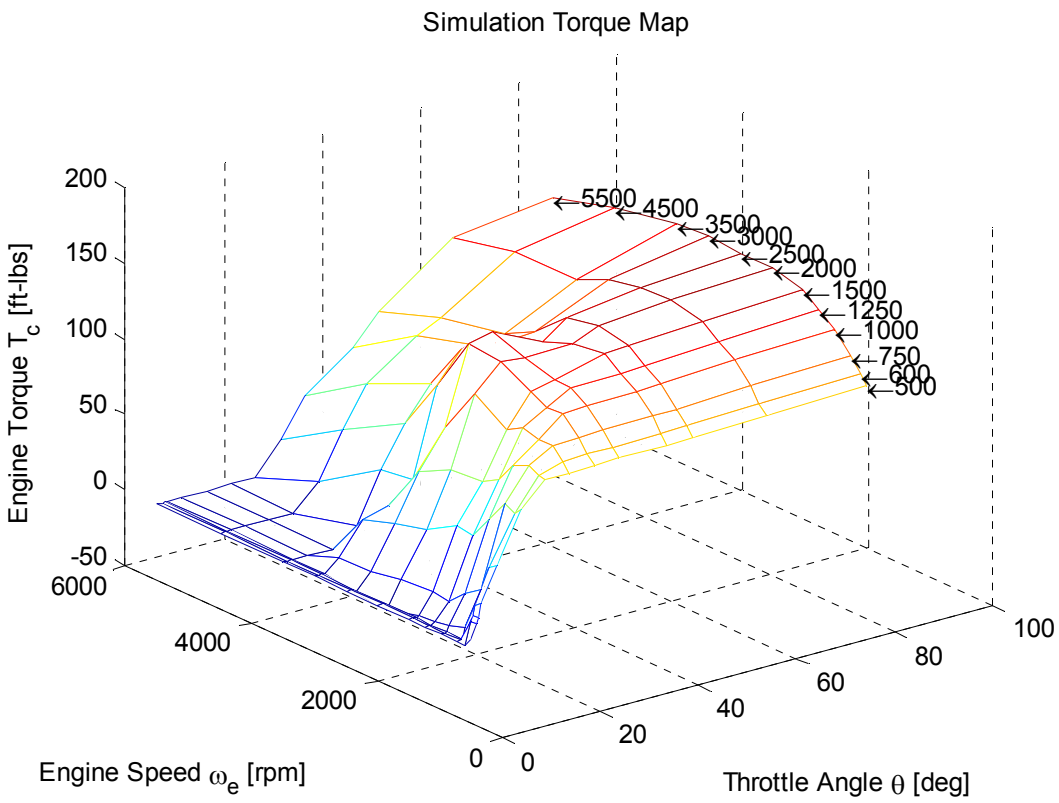

Figure 42 Simulation torque map

The torque map has been used to speed up the computations of engine torque. The frictional and load torque as well as the torque due to the pump (from torque converter) act against the torque produced by the engine and the resultant torque turns the crankshaft and the output is the engine speed.

6.2.2. Torque Converter Dynamics Model

The torque converter is modelled using sets of two quadratic equations. The correct set of equations is selected depending on the speed ratio which is given by:

$$SR = \frac{w_t}{w_e}$$

The torque converter produces an output torque called the "Turbine Torque" T_t which is then passed through the gear selection and reduction block inside the transmission model block.

The feedback from the torque convertor is obtained as "Pump Torque" T_p which is feedback to the engine.

The sets of quadratic equations used to model the torque convertor are given below.

Convertor mode: ($SR < 0.842$)

$$T_p = 0.3205 \cdot 10^{-4}\omega_e^2 + 0.0196 \cdot 10^{-4}\omega_e\omega_t - 0.2359 \cdot 10^{-4}\omega_t^2$$

$$T_t = 0.7313 \cdot 10^{-4}\omega_e^2 - 0.6413 \cdot 10^{-4}\omega_e\omega_t - 0.0388 \cdot 10^{-4}\omega_t^2$$

Coupling mode: ($0.842 \leq SR \leq 1$)

$$T_p = -0.0612 \cdot 10^{-3}\omega_e^2 + 0.2612 \cdot 10^{-3}\omega_e\omega_t - 0.2009 \cdot 10^{-3}\omega_t^2$$

$$T_t = -0.0612 \cdot 10^{-3}\omega_e^2 + 0.2612 \cdot 10^{-3}\omega_e\omega_t - 0.2009 \cdot 10^{-3}\omega_t^2$$

Overrun mode: ($SR > 1$)

$$T_p = -0.1791 \cdot 10^{-4}\omega_e^2 - 0.2135 \cdot 10^{-4}\omega_e\omega_t - 0.0344 \cdot 10^{-4}\omega_t^2$$

$$T_t = -0.1791 \cdot 10^{-4}\omega_e^2 - 0.2135 \cdot 10^{-4}\omega_e\omega_t - 0.0344 \cdot 10^{-4}\omega_t^2$$

6.2.3. Transmission Model

The transmission block consists of a gear selection block which desides which gear is to be selected depending on the throttle angle θ and transmission output speed ω_T in rpm. The transmission output speed is measured before final gear reduction. The individual gear ratios are listed in table 2 below.

Gear	Gear Ratio	Gear Ration w/ Final Reduction
1st	2.705:1	11.590:1
2nd	1.482:1	6.350:1
3rd	1.057:1	4.529:1
4th	0.707:1	3.029:1
Rev	2.047:1	8.770:1
Final Reduction	4.285:1	

Table 2. Transmission gear ratios

The logic to select the correct gear depends upon the set of linear curves for gear changes given in Figure 43.

Depending on which gear the vehicle is, the corresponding gear reduction is applied to the turbine torque.

6.2.4. Longitudinal Drive-train Dynamics Model

The vehicle model gives us the output vehicle speed ω_v in ft/sec. It accounts for the rolling resistance, torque due to road inclination, torque due to air resistance, any other load disturbances and braking torque.

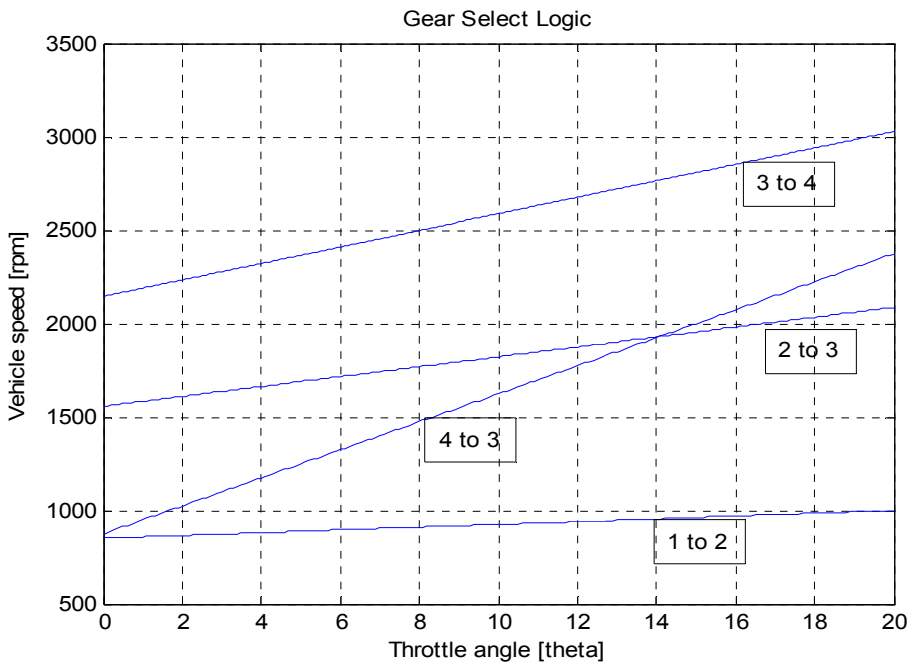

Figure 43 Gear shift pattern

The vehicle dynamics are modeled as shown below.

$$\dot{V} = \frac{r}{M_v}(G_T T_t(\omega_e, \omega_t) - \gamma V^2 - T_{rr} - T_b)$$

where V = vehicle velocity (ft/sec)

r = radius of tire (ft)

M_v= vehicle mass (slugs)

G_T= overall transmission gear ratio

T_t= torque from transmission (ft.lbs)

γ = aerodynamic drag coefficient

T_{rr}= rolling resistance (ft.lbs)

T_b= braking torque (ft.lbs)

The vehicle mass is taken to be 130.578$slugs$, tire radius to be 1ft, aerodynamic drag coefficient to be 0.0117 $1/ft$ and rolling resistance to be 59.2 $ft.lbs$.

6.3.Master Speed Controller

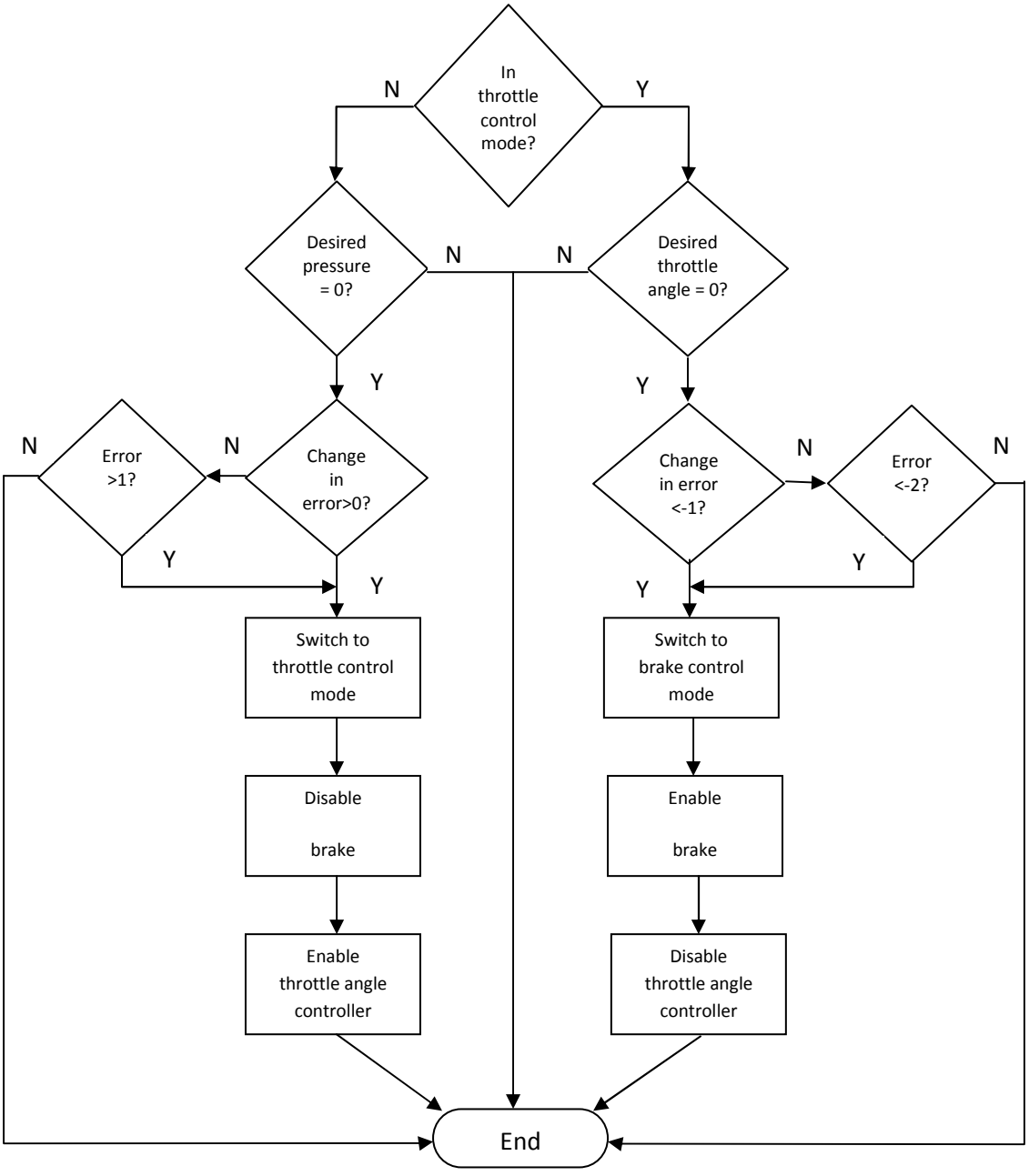

Figure 44 Flow chart indicating decision paths of master speed controller

The master speed controller is used to select between two modes of operation- throttle control mode and brake control mode depending on the error between the desired vehicle speed and the actual or estimated vehicle speed. The flow chart for used is shown below in Figure 44.

6.4.Simulation Results of Vehicle Dynamics of Longitudinal Model

The simulation results of the internal vehicle dynamics is shown in Figure 45. A reference velocity of 45 mph is given to the vehicle and plots for vehicle measured speed, estimated speed, engine speed, throttle angle, brake pressure, gear and speed ratio of torque convertor are given.

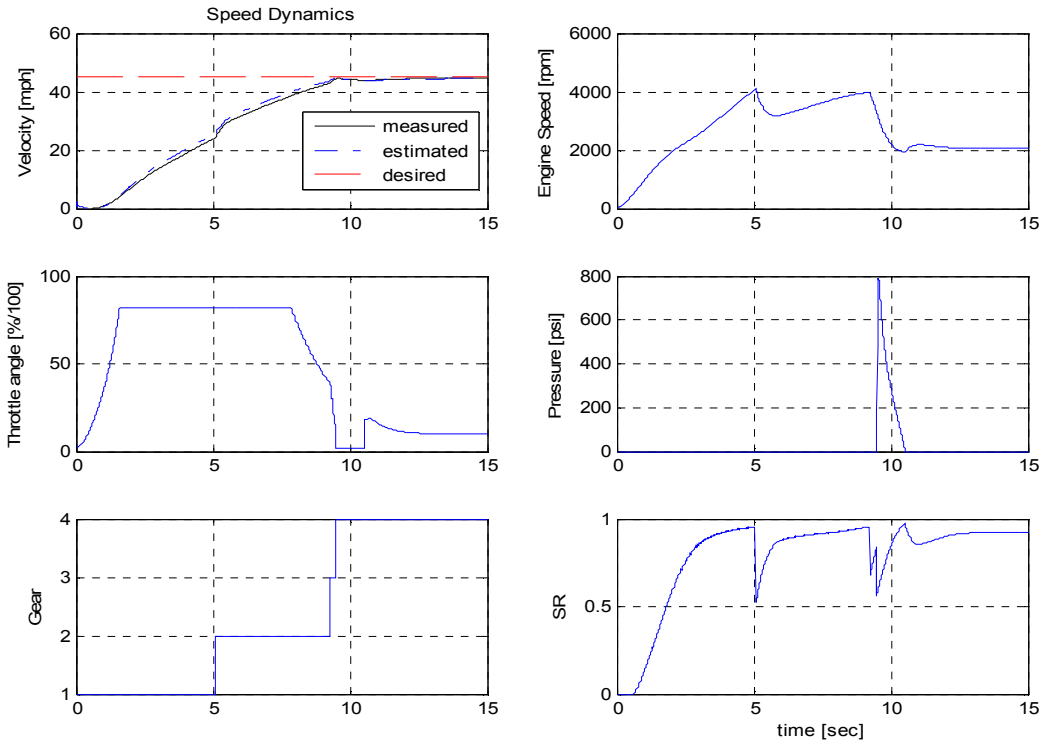

Figure 45 Results of internal vehicle dynamics

In this appendix we have given a brief introduction of the model we are going to use for simulations on the two GCDC scenarios.

BIBLIOGRAPHY

[1] Bender J. G., Fenton R. E. and Olson K. W. (1971). "An Experimental Study of Vehicle Automatic Longitudinal Control." *IEEE Transactions on Vehicle Technology* , VT-20, 114-123.

[2] "Studies in vehicle automatic longitudinal control." Tech Rep. Report Es 267A - 7 prepared under Contract to the Ohio Department of Highways and U. S. Bureau of Public Roads, Dept. of Electrical Engineering, The Ohio State University

[3] R. L. Cosgriff, et. al., "An automated system for longitudinal control of vehicles." Highway Res. Rec.,no. 122, pp 7 - 18, 1966.

[4] Desoer, S. S., "Longitudinal control of a platoon of vehicles with no communication wth the lead vehicle information." *Proceedings of the American Control Conference*, pp. 3102-3106, 1991.

[5] D. H. McMohan, J. K. Hedrick, and S. E. Schladover, "Vehicle modeling and control of automated highway systems." *Proceedings of American Control Conference*, pp 297-303, 1990.

[6] J. K. Hedrick, D. McMohan, V. Narendran, and D. Swaroop, "Longitudinal vehicular control design for IVHS systems." *Proceedings of the American control Conference*, pp 3107 - 3112, 1991.

[7] Martin Sommerville, " Implementation of a longitudinal Controller for use on an Automated Highway System." Master's Thesis, The Ohio State University. Spring 1996.

[8] Umit Ozguner "Autonomy in Vehicles." Course Notes for 753.02 Spring quarter 2010.

[9] W. S. Levine and M. Athans, "On the optimal error regulation of a string of moving vehicles." *IEEE Transaction on Automatic Control*, Vol. AC-11, No. 3, pp 355 - 361, July 1966.

[10] U. Ozguner and W. R. Perkins, "Optimal control of multilevel large-scale systems." *Int. J. Control*, Vol.28, No. 6, pp 967-980, 1978.

[11] Martin Sommerville, Cem Hatipoglu, Umit Ozguner, "Switching control of a pneumatic throttle controller." Control Systems Magazine, IEEE,Vol. 18, No. 4, pp 81-87,Aug 1998.

[12] Robert E. Fenton and Robert J. Mayhen, "Automated Highway Studies at The Ohio State University - An Overview." *IEEE Transactions on Vehicle Technology* , Vol. 40, No. 1 pp. 100-113, Feb 1991.

[13] D. F. Wilke "A moving cell control scheme for automated transportation systems." Transportation Sci., vol 4, pp 347 - 364, Nov 1970.

[14] Gerald M. Takasaki and Robert E. Fenton, "On the identification of vehicle dynamics." *IEEE Transaction on Automatic Control*, Vol. AC-22, No. 4, pp 610 - 615, Aug 1977.

[15] H. Raza and P. Ioannou, "Vehicle following control design for automated highway systems." California PATH Research Report 1997, UCB-ITS-PRR-97-2.

[16] Robert J. Hansen "Planning for high-speed ground transportation." Proceeding of IEEE, Vol 56, No. 4, April 1968

[17]P. A. Ioannou, F. Ahmed-Zaid, D. H. Wuh, "A time headway autonomous intelligent cruise controller: Design and simulation." California PATH Working Paper 1997, UCB-ITS-PWP-94-07

[18] Cem Hatipoglu and Martin Sommerville, "Development of Computationally Efficient Time-Domain Engine Model." Control Research Lab, The Ohio State University, Report 96-02, February 1996.